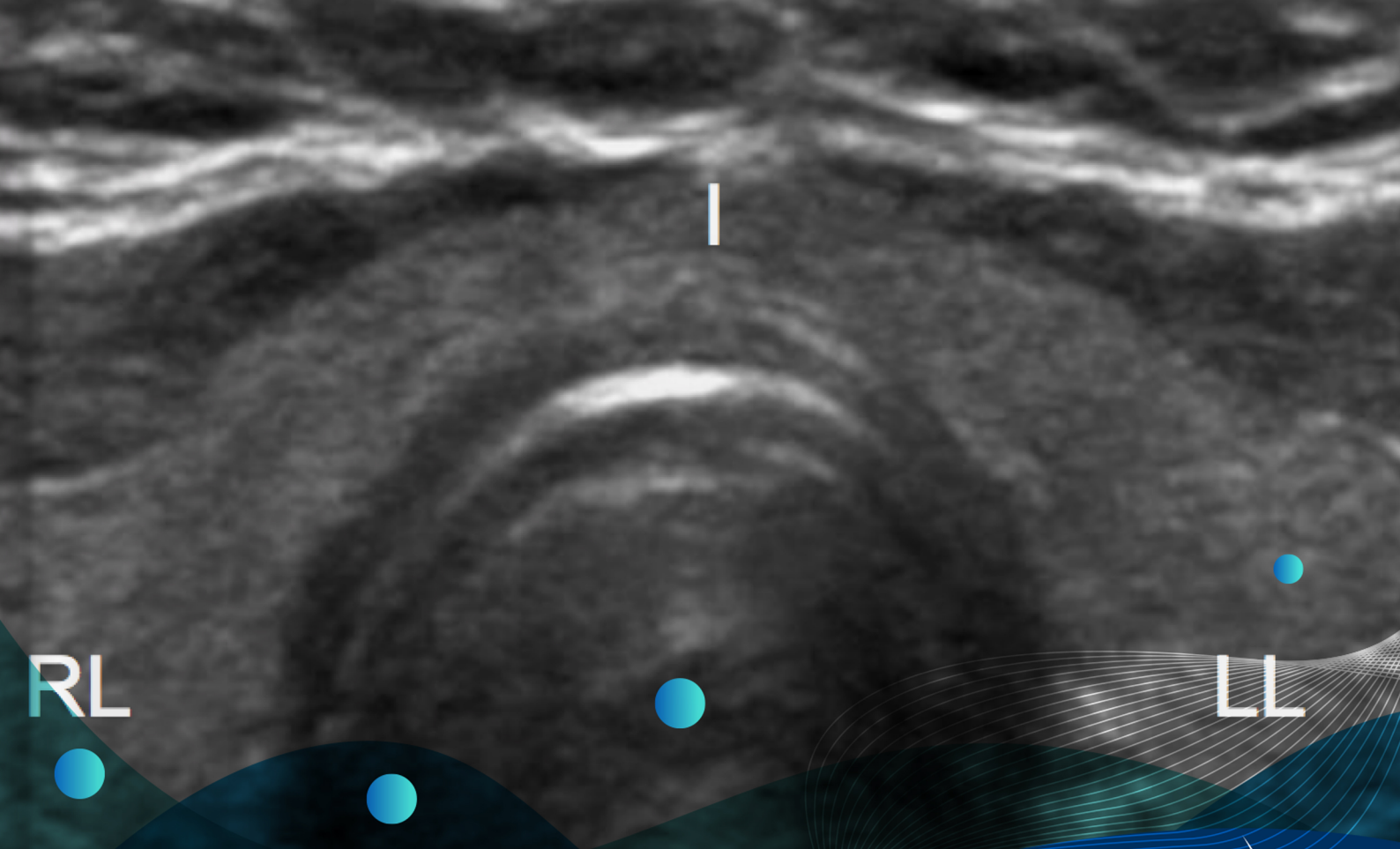


EFSUMB
European Federation of Societies for Ultrasound in Medicine and Biology

# EFSUMB Course Book

2nd Edition

**Editor: Christoph F. Dietrich**

## Ch18: Ultrasound of the thyroid

*Nira Beck-Razi[1], Diana Gaitini[1], Rhodri M Evans[2], Gordana Ivanac[3], Christoph F Dietrich[4]*

*1. Department of Medical Imaging, Rambam Health Care Campus and Faculty of Medicine, Technion, Haifa, Israel.*
*2. Department of Diagnostics, Abertawe Bro Morgannwg University Health Board, Wales, England.*
*3. Department of Diagnostic and Interventional Radiology, Dubrava University Hospital and Medical School, University of Zagreb, Zagreb, Croatia.*
*4. Department Allgemeine Innere Medizin, Kliniken Beau Site, Salem und Permanence, Hirslanden, Berne, Switzerland*

*Corresponding author: Nira Beck-Razi*
*Department of Medical Imaging, Rambam Health Care Campus and Faculty of Medicine, Technion, Haifa, Israel*
*Email: n_beck_razi@rambam.health.gov.il*
*Acknowledgement: The authors thank Professor Dr. Anthony Rudd for review. The authors thank Rhodri M Evans who contributed to the first edition of the EFSUMB Course Book.*

## Introduction

High-resolution ultrasound is the most sensitive imaging test available for the examination of the thyroid gland. It is used to detect thyroid lesions, accurately calculate their dimensions, identify the internal structure and vascularisation and evaluate diffuse changes in the thyroid parenchyma. Thyroid ultrasound is able to confirm the presence of a thyroid nodule when physical examination is equivocal. It can differentiate between thyroid nodules and cervical masses from another origin, such as cystic hygroma, thyroglossal duct cyst and lymphadenopathy. Thyroid ultrasound is able to detect thyroid nodules in unusual clinical scenarios such as patients with a history of head and neck radiation, multiple endocrine neoplasia (MEN) Type II, and to diagnose lymphadenopathy in jugular, submandibular and supraclavicular chains.

## Clinical indications

Indications for thyroid ultrasound follow the American Association of Clinical Endocrinologists recommendations and many other guidelines and recommendations and are summarised in the following list [(1)].

## Role of thyroid ultrasound

There are three main roles of thyroid ultrasound:

1. To detect thyroid and cervical masses, including relapse in the thyroid bed and cervical adenopathy after thyroidectomy.
2. To differentiate between possible benign and probably malignant masses based on their sonographic appearance.
3. To guide the performance of fine-needle aspiration (FNA) biopsy and percutaneous treatment.
4. Use as a screening test in the general population for thyroid cancer

Thyroid ultrasound can provide the answers to several clinical questions:

1. Is the palpable mass within or adjacent to the thyroid?
2. Is the tumour confined to the thyroid or does it locally invade nearby structures?
3. Are cervical lymph nodes involved?
4. Is there a primary focus in the thyroid gland of a patient with cervical adenopathy?
5. Is there a post-operative residual or recurrent tumour in the thyroid bed or metastases to neck lymph nodes?

## Technical guidelines

The patient should be examined supine with the neck hyperextended (a pillow may be placed below the shoulders to achieve this). A high-frequency linear transducer (7–15MHz) [Figure 1] is used to provide enough penetration (approximately 5cm depth) and excellent resolution (0.7–1mm). This level of resolution is not achieved by any other imaging method. Images are performed on greyscale and colour Doppler.

**Figure 1 High-resolution linear transducer (7–15MHz) for of thyroid sonography.**

The recommended protocol for thyroid ultrasound is in the American College of Radiology Practice Guideline [(2)], which is as follows:

1. Transverse scans of the whole gland at the upper, mid and lower poles and the isthmus, and side-by-side images of each lobe, to compare echogenicity and size of both lobes. Each lobe width and anteroposterior diameters are measured [Figure 2a].
2. Longitudinal scans through each lobe on medial, mid and lateral planes. The length of the lobes is measured [Figure 2b].
3. Identify focal lesions, measure the main lesions and identify the dominant one (according to size).
4. Document the presence of enlarged lymph nodes or thrombosed jugular vein.

Standardised ultrasound reporting criteria should be followed indicating the position, shape, size, margins, content, echogenicity and vascular pattern of the whole gland and, when present, the focal lesions. Nodules with malignant potential should be identified and FNA biopsy should be suggested to the referring physician.

**Figure 2 Thyroid measurement on (a) transverse and (b) longitudinal scans.**

a


b


## Normal anatomy

The normal thyroid is comprised of two lobes and the isthmus, which bridges the lobes in front of the trachea. Size and shape are variable depending on the age of the patient (Table 1). It has a medium to high-level echogenicity. The relationships with the surrounding structures are as follows: ahead, the strap muscles and sternocleidomastoid muscle; behind, the trachea and longus colli muscles bilaterally, the common carotid artery and jugular vein and finally, the oesophagus lies behind the left thyroid lobe [Figure 3].

**Table 1 Normal thyroid dimensions. A-P, anteroposterior; SD, standard deviation**

| Age | Longitudinal | A-P | Volume | Isthmus |
|---|---|---|---|---|
| Newborn | 18-20 mm | 8-9 mm | | |
| 1 year old | 25 mm | 12-15 mm | | |
| Adult | 40-60 mm | 13-18 mm (up to 20 mm) | 18.6 mL or gram (SD:4.5)<br>M: 19.6 (4.7)<br>F: 17.5 (4.2) | 4-6 mm A-P |

**Figure 3 Normal thyroid and surrounding structures on transverse scans. RL, right lobe; LL, left lobe; I, isthmus; E, esophagus; T, trachea; SM, strap muscles; SCM, sternocleidomastoid muscle; JV, jugular vein; CCA, common carotid artery.**

a

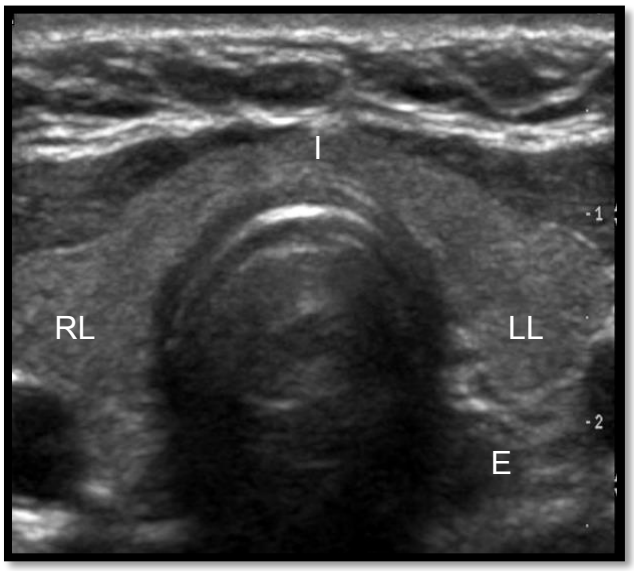


b

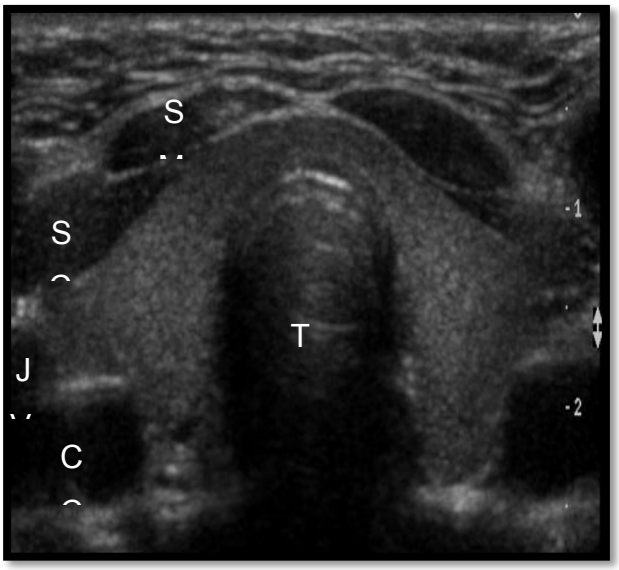


Colour and power Doppler ultrasound are useful in the evaluation of vascularity of the thyroid gland and focal masses. The thyroid gland is a richly vascularised organ. The arterial supply is provided on each side by the superior thyroid artery (a branch of the external carotid artery) and the inferior thyroid artery (a branch of the thyrocervical trunk, which is a

branch of the subclavian artery). The thyroid arteries may be localised on colour or power Doppler. Low-resistance flow is demonstrated on spectral Doppler in these visceral arteries. A peak systolic velocity in the intra-thyroid arteries is in the range of 15–30cm/s and is the highest velocity found in any superficial organ [Figure 4].

**Figure 4** **Arterial vascularisation of the thyroid gland. On colour Doppler imaging the inferior thyroid artery is seen (a). On spectral display a low-resistance flow with a high systolic velocity is obtained (b).**

a

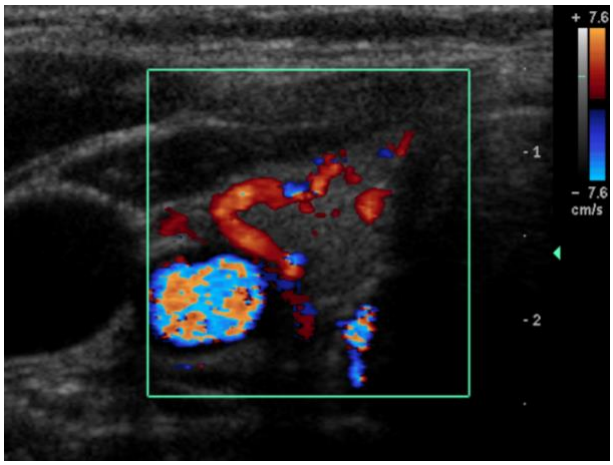


b

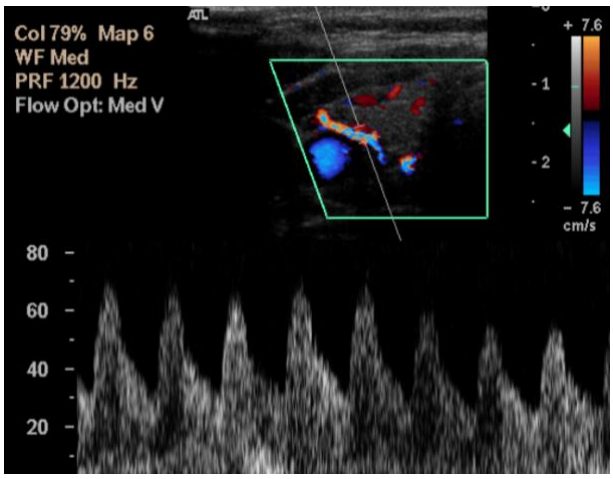

## Congenital anomalies

Congenital agenesis or hypoplasia of the thyroid gland may include the whole gland or just one of the lobes. The aortic sac of the heart descends and pulls the thyroid caudally from its origin at the base of the tongue [Figure 5], its pharyngeal connection elongates as a stalk (the thyroglossal duct), which normally disappears in the fifth to sixth week of intrauterine life. Ectopic thyroid, a deficit in migration of the thyroid gland to the lower neck, commonly develops at a sublingual or a suprahyoid position. Ectopic thyroid can be easily detected on radionuclide scans [Figure 6].

**Figure 5** **Congenital developmental defects and clinical outcomes. Development of the thyroid gland begins in the first and second weeks of intrauterine life and is complete by week 11. The thyroid gland arises as an endodermal thickening at the junction of the developing anterior and posterior tongue, at the level of the foramen caecum, between the first and second branchial arches (from [] Mewly J et al, Radiographics 2005;25:931-948, with permission).**

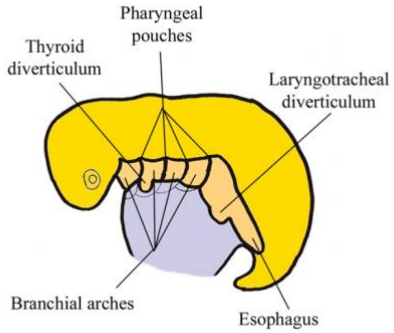

**Figure 6 Ectopic (sublingual) thyroid seen on thyroid scintigraphy ($I^{123}$).**

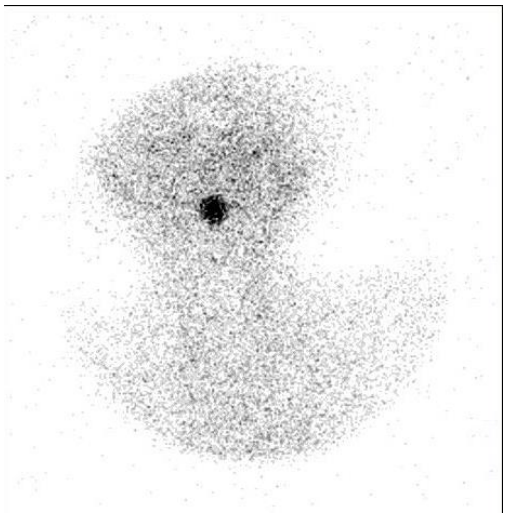

A thyroglossal cyst, forming from a persistent thyroglossal duct, appears as a neck lump in the midline [Figure 7]. A normally positioned thyroid gland must be examined to exclude thyroid agenesis. In the absence of a normal thyroid the cyst will be the only thyroid tissue present.

**Figure 7 Midline neck lump in a 2 year old male. Normal thyroid gland at the base of the neck is present (a). A cyst (cursors) is seen ahead of the isthmus of the gland. The cyst (arrow) is demonstrated between the thyroid isthmus and the hyoid bone (b). The submandibular salivary gland (SG) is shown above the cyst. A thyroid radionuclear scan was performed pre-operatively to confirm that the thyroid gland was present and functioning normally.**

a


b

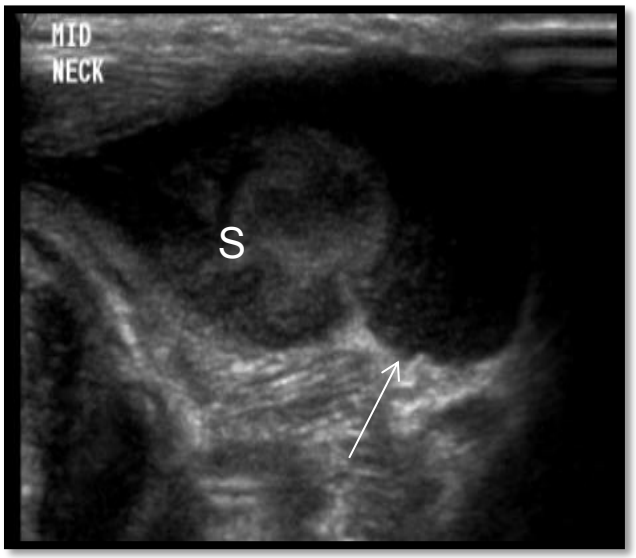


## Benign thyroid nodules

### Nodularity

The development of nodules can be regarded as a normal part of the maturation process of the thyroid. The incidence correlates directly with age [Figure 8].

**Figure 8 Incidence of thyroid nodules (*y*) at ultrasound (US)/autopsy and on palpation related to patient age (3).**

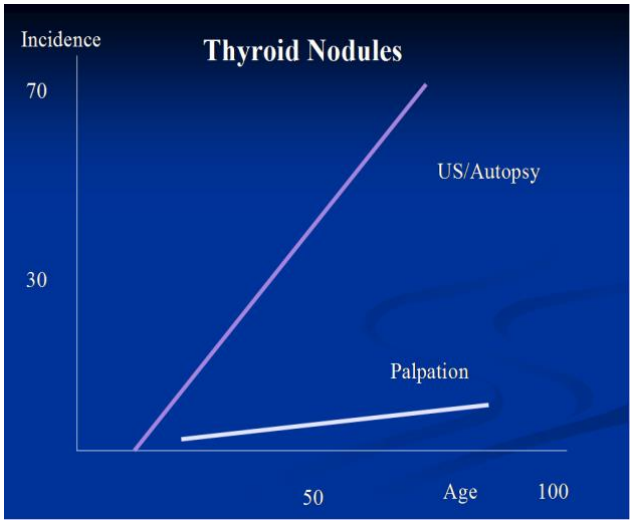


Ultrasound is an extremely sensitive tool for the detection of nodules and is equal to that of pathologists at post-mortem. There is a 30–70% incidence of thyroid nodules on ultrasound examination, depending on the age of the patient population. However, while the incidence of nodularity within the thyroid is high, the incidence of thyroid cancer is low. In the United Kingdom, the quoted incidence of thyroid carcinoma is 1 per 50000 patients per annum. Therefore, a radiologist or thyroid surgeon working in a large hospital with a catchment population of 500,000 patients would expect to see only 10 new cases of thyroid cancer a year. However, a radiologist could reasonably expect to see thyroid nodules in approximately half of the patients scanned each year. The dilemma for the radiologist or sonographer is how to identify the few thyroid cancers present within a multitude of benign thyroid nodules.

Fortunately, there are some well-documented signs that can be used in the differentiation of benign from malignant thyroid nodules on ultrasound. Thyroid nodules are formed as a result of hyperplasia and involution within the thyroid. These hyperplastic nodules frequently undergo a process of cystic degeneration *i.e*. they contain cystic areas as they mature. As the nodules evolve, haemorrhage may occur within the nodule that can increase the cystic component [Figure 9].

**Figure 9 Thyroid nodularity. Normal thyroid with an uncommon absence of nodules (a). Iso- and hyperechoic benign thyroid nodule with a halo present and cystic degeneration (b).**

a

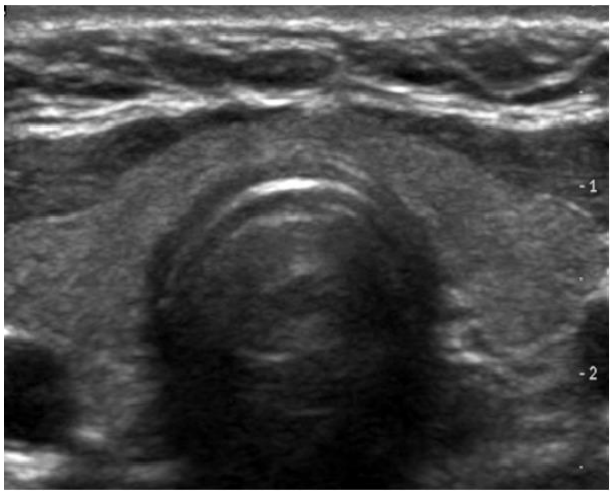

b

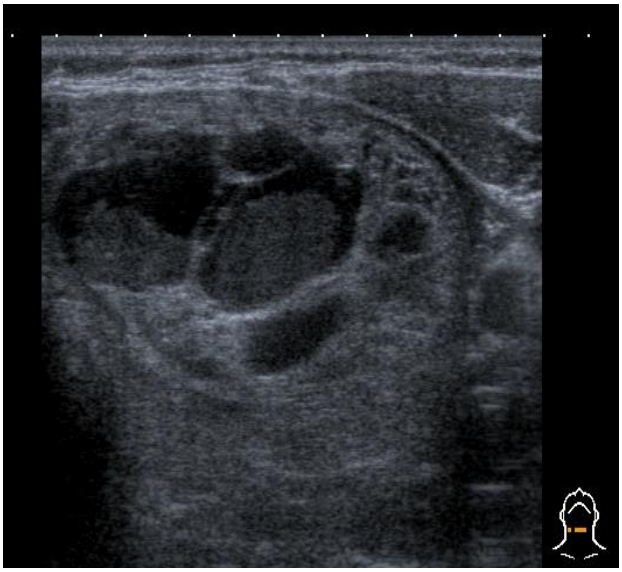

**Ring down or Comet tail sign of colloid**

A major constituent of benign thyroid nodules is colloid. Colloid causes a “ring down” or "comet tail" artefact or sign, typically within the cystic element of a nodule. Ahuja et al [(4)]

were the first to describe this sign on ultrasound. When seen, it identifies the presence of colloid within a nodule and implies that this is a benign colloid nodule [Figure 10].

**Figure 10 "Ring down" sign within the solid component of a cystic colloid nodule.**

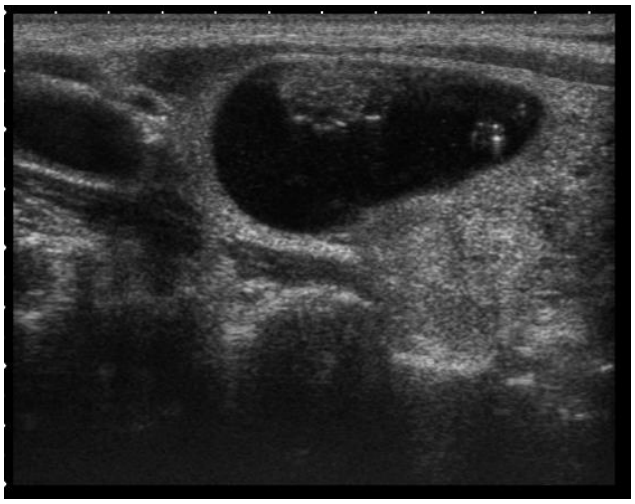

Care needs to be taken by the operator to ensure that the echogenic ring down sign is not mistaken for the microcalcification that is pathognomonic of papillary carcinoma of the thyroid. Operators need to be aware of the various software applications present in modern ultrasound machines that can impair the detection of microcalcification and the colloid ring down sign. The ring down sign is also frequency dependent. It is good practice to have multiple pre-sets on your machine to allow the user to review equivocal nodules and signs with and without the various processing software applications.

**Calcification**

It was previously agreed upon that microcalcifications have a known association with thyroid malignancy while a peripheral or eggshell calcification within a thyroid nodule indicates that it is benign. However, several recent investigators suggested that detection of macrocalcification as well as microcalcification should raise the suspicion for thyroid carcinoma [(5-9)] [Figure 11].

Occasionally, large aggregates of calcification are identified within benign thyroid nodules. It is thought that this may occur following hemorrhage within a nodule.

**Figure 11 Patterns of calcifications in a thyroid nodule. Typical benign peripheral or "egg shell" calcification (arrow) (a). Solid hypoechoic lesion containing microcalcifications with a diagnosis of papillary carcinoma (b).**

a

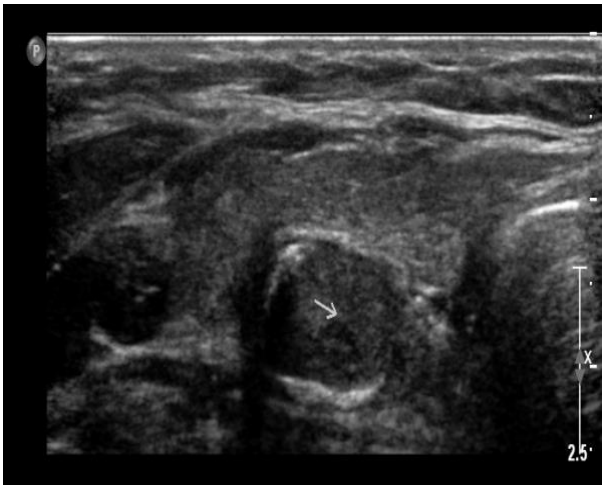


b

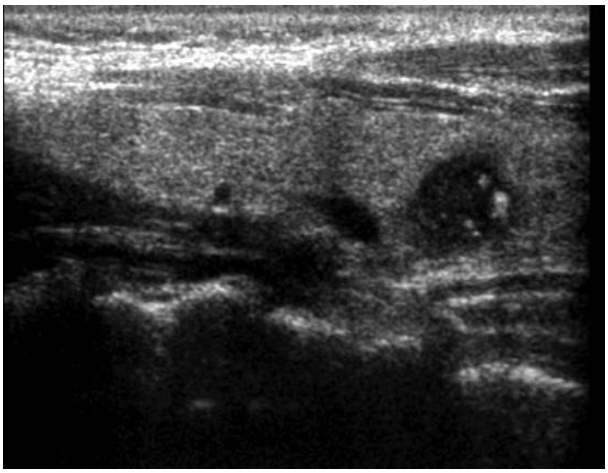

## Echogenicity

The majority of benign thyroid nodules will be iso- or hyperechoic relative to the normal “background” echo-texture of the thyroid. If a solid thyroid lesion is hyperechoic relative to normal thyroid tissue the reported incidence of malignancy is only 4% [(10)]. If the lesion is isoechoic the incidence of malignancy increases to 26% and there is a 63% malignancy of hypoechoic nodules. A significantly hypoechoic (more hypoechoic than the strap muscles) solid lesion should always be viewed with suspicion [Figure 12].

**Figure 12 Benign nodule. Hyper - or isoechoic to background echo-texture. A cystic change is common (a). Malignant nodule - Papillary carcinoma. Hypoechoic to background echo-texture (arrow) (b).**

a

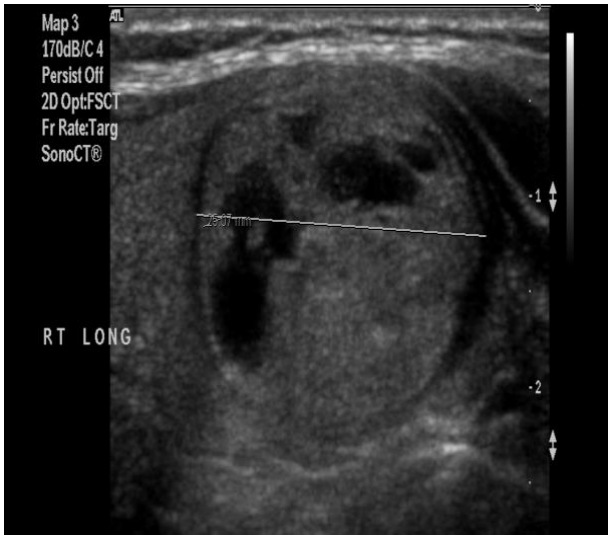


**Multiplicity of nodules**

Is the presence of multiple nodules an indicator that they are benign? In three of the largest studies [(11-13)], on the use of thyroid ultrasound in the detection of malignancy, the incidence of malignancy in solitary nodules compared with multiple nodules is similar [Table 2], [Figure 13].

**Table 2 Incidence of thyroid carcinoma**

| Reference | Solitary (%) | Multiple (%) |
|---|---|---|
| Cochand et al. (14) | 13 | 14 |
| Marqusee et al. (15) | 7 | 9 |
| Papini et al. (16) | 9 | 6 |

**Figure 13 Multiple colloid nodules within the thyroid. Note the ring down sign.**

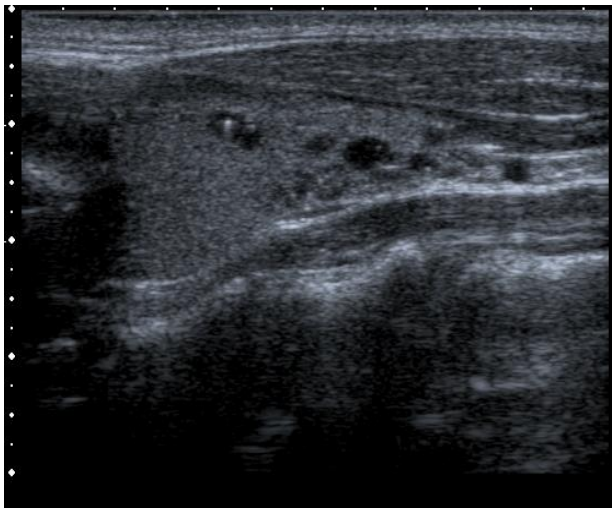

Thus, we can say that the presence of multiple nodules within a thyroid cannot be taken as an indicator that the lesions are benign. When a suspicious nodule is discovered incidentally in the thyroid, FNA should be performed in this nodule even if the patient was referred for another palpable lesion [Figure 14].

**Figure 14 Incidentally discovered papillary carcinoma in a 70-year-old female referred to thyroid sonography for a palpable nodule at the isthmus. An oval well-defined nodule with a hypoechogenic halo is seen at the isthmus, which corresponds with the clinical finding (a). On transverse (b) and longitudinal (c) scans, a hypoechogenic ill-defined nodule (arrow in b) is seen in the right lobe on transverse and longitudinal scans, which is highly suspicious for malignancy. Fine-needle aspiration from the suspicious nodule was performed (small arrow) and papillary carcinoma was diagnosed on cytology (d).**

a

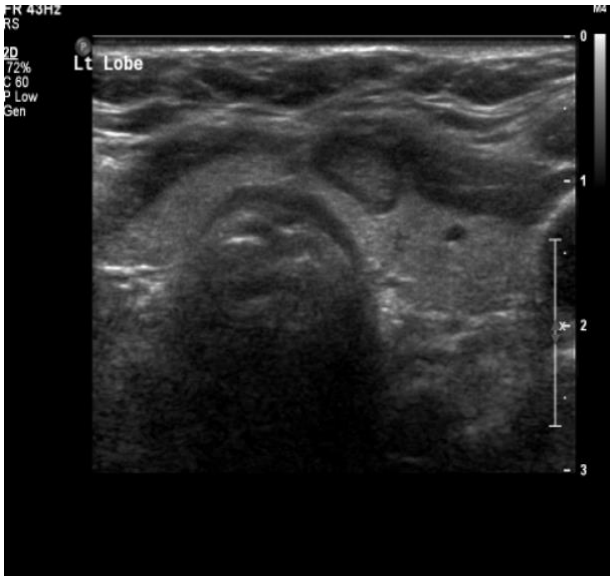


b

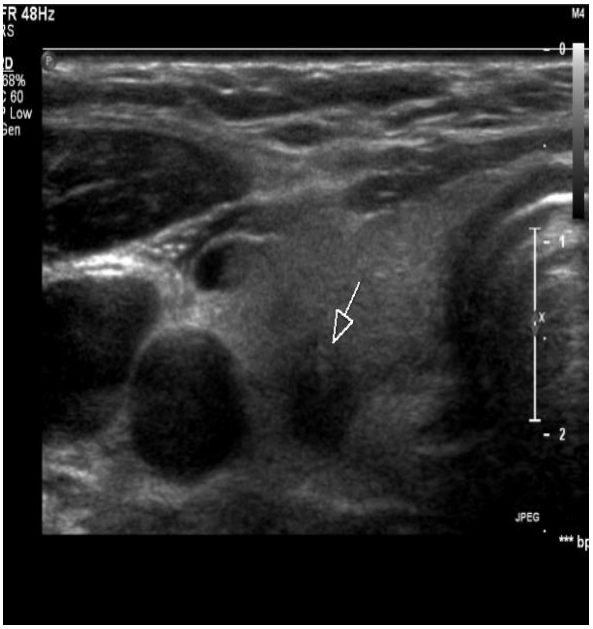


c

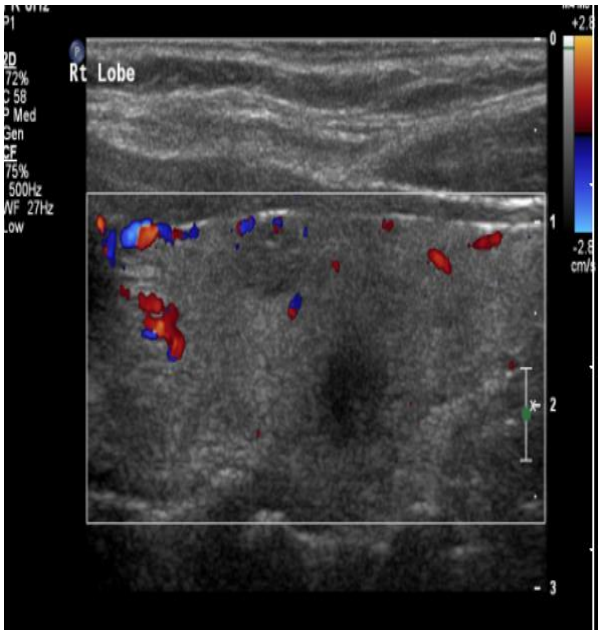


d

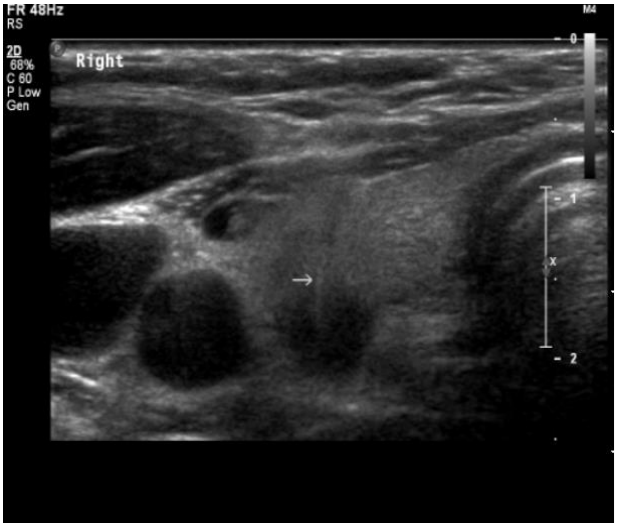


**Halo/margin/shape**

The margin of the thyroid nodule should be reviewed as part of ultrasound assessment. In benign nodules a hypoechoic halo is typically identified surrounding hyper or iso-echoic nodules. This “halo” is caused either by the capsule of the nodule or is due to adjacent compressed thyroid tissue. Some studies have shown that the presence of a halo infers the nodule is benign. A complete halo has been reported to be 12 times more likely to indicate the nodule is benign rather than malignant [Figure 15]. As with all signs, the halo sign is not

an absolute indication of that it is benign because it may be seen in thyroid malignancy [(17)]. If, as stated, the sign is a result of adjacent compressed thyroid tissue it is not surprising that, given the indolent nature of papillary carcinoma, there will be adjacent compressed thyroid tissue that could manifest itself as a halo surrounding a papillary carcinoma. A malignant lesion is more likely to appear with irregular margins. Furthermore, a shape that is taller than wide of the thyroid nodule has been shown to correlate with thyroid cancer. Moon HJ et. al. demonstrated that taller than wide shape in either the tranverse or longitudinal plane was useful to predict malignancy [(18)]. However, Tessler and colleagues emphasized the need to evaluate the shape in an axial plane [(2)] [Figure 15 and 16].

**Figure 15 Halo surrounding a hyperechoic homogenous lesion-follicular lesion.**

**Figure 16 A taller- than- wide nodule, papillary carcinoma on cytology.**

## Colour flow patterns

The last feature to discuss when considering benign thyroid nodules is the colour flow patterns detected on colour flow imaging. Assessment of colour flow should be an adjunct to the spectrum of signs that help in the differentiation of benign from malignant nodules. The operator should ensure the machine is set-up with a readily available preset to detect low/medium velocity flow within nodules with little motion artefact. Standard colour flow assessment or power Doppler assessment can be used. The principle is the detection of a flow pattern rather than the direction of flow. This author (RE) advises adjusting the colour flow parameters to detect flow within the lingual artery, deep to the hyoglossus muscle. Once the parameters are set for this flow velocity it is usually a satisfactory preset for colour flow assessment within a thyroid nodule.

Originally three colour flow patterns were described within thyroid nodules [(19)]: Type I, no flow detected within the nodule; Type II, perinodular arterial flow pattern; and Type III, intranodular flow with multiple vascular poles, chaotic arrangement, with or without perinodular flow.

Type I and II are mostly seen in benign hyperplastic nodules, whereas Type III is generally identified in malignant nodules.

Given the high colour sensitivity of modern ultrasound machines, vessels are now detected within the majority of thyroid nodules. It is probably easier to think in terms of predominantly peripheral flow as typical of a benign colour flow pattern [Figure 17a] whereas a chaotic intranodular pattern is more indicative of malignancy [Figure 17b].

**Figure 17 Benign colour flow pattern. Note the hyperechoic nodules relative to the thyroid, the halo and peripheral colour flow with no significant intranodular flow (a). Malignant intranodular chaotic blood flow pattern (b).**

a

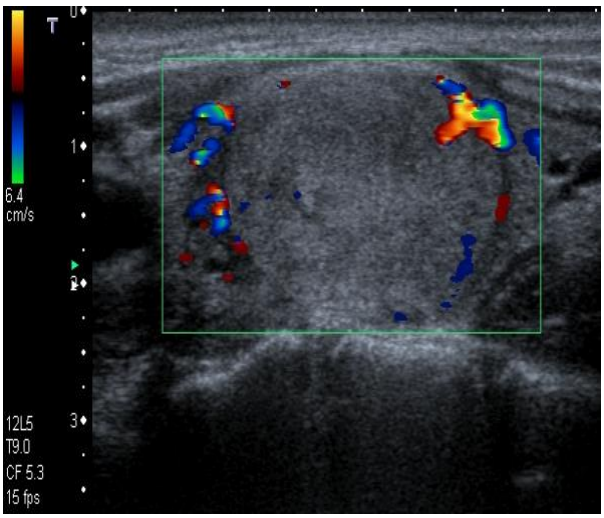


b

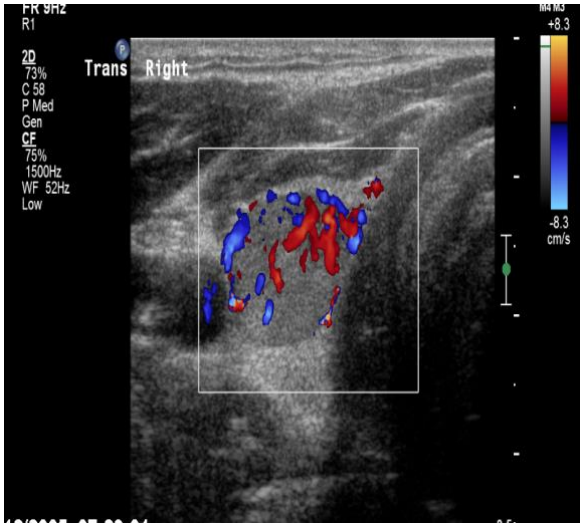

## Malignant thyroid nodules

Thyroid cancer represents less than 1% of all malignancies. There is an average annual incidence of 5 per 100000 people. The incidence of thyroid cancer in the United States increased from 3.6 per 100 000 in 1973 to 8.7 per 100 000 in 2002, which is a 2.4–fold increase [(20)]. Mortality from thyroid cancer is approximately 0.5 per 100 000 with a 4–8% 20 years cumulative mortality. This was stable between 1973 and 2002, which suggests that changes in the diagnostic approach to thyroid nodules resulted in an increased detection of the sub-clinical disease [(20)].

The incidence of cancer in thyroid nodules is low (10–13%) with the same incidence between occult and palpable nodules [(21, 22)]. Thyroid cancer is more frequent in females and has two peaks of prevalence: the first under 20 year of age and the second in patients over 60-year-old. Histologically, 75–80% are papillary or mixed papillary and follicular; 10–20% are follicular, 3–5% are medullary and 1–2% are anaplastic carcinomas. Two histological types, papillary and follicular, are included in the subgroup of differentiated thyroid carcinoma (DTC).

Thyroid cancer first spreads to the lymphatic cervical nodes. Distal metastases are infrequent and occur in 2–3% of cases, mostly to bones and lungs.

### Papillary carcinoma

The described sonographic appearance of thyroid cancer is related to the most frequent histological type *i.e.* the papillary carcinoma [Table 3].

The malignant nodule echogenicity as seen on B-mode greyscale is low in 90% of cases. Microcalcifications, with or without acoustic shadow, when present, are a reliable diagnostic criterion. Hypervascularity with a disorganised pattern is seen on colour Doppler sonography in 90% of cases [Figure 18].

**Figure 18 Incidentally discovered papillary carcinoma in a 54-year-old female during carotid ultrasound Doppler examination. A hypoechogenic nodule with a**

**poorly-defined margin and without a surrounding halo is detected in the right thyroid lobe (a). Microcalcifications without acoustic shadowing are seen (arrowheads) (b).**

a

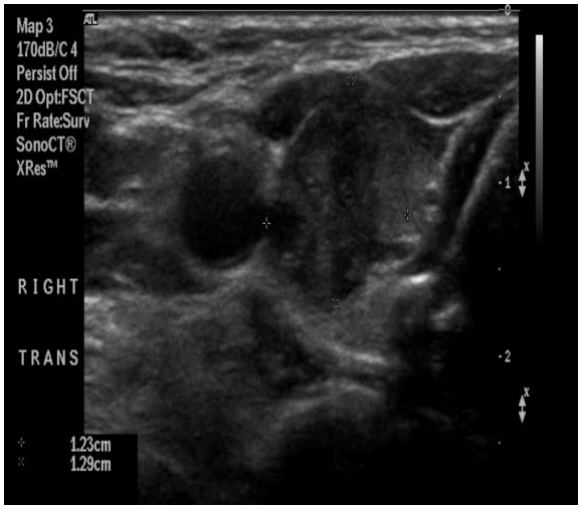


b

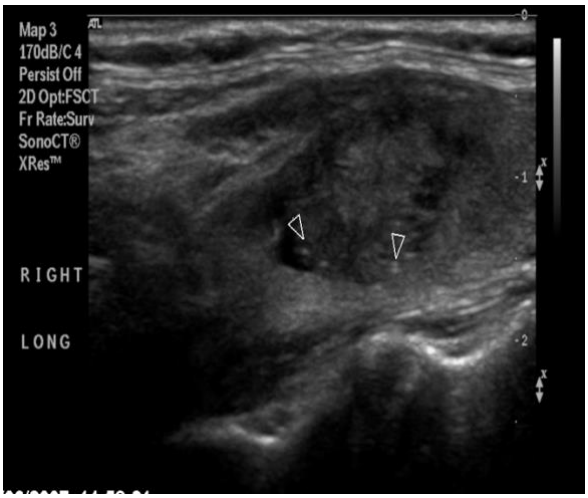


***Cervical lymph nodes in papillary thyroid cancer***

Despite the indolent nature of papillary carcinoma, thyroid cervical lymph node involvement is common and the cervical lymph nodes must be systematically searched for. The location of cervical lymph nodes has been classified by the American joint committee on cancer according to specific nodal stations [Figure 19]. The most important nodes that need to be evaluated are the lateral cervical chain; levels II-V. Level I nodes are the submental and

submandibular nodes. Level II are located at the upper internal jugular chain, level III are located in the mid – internal jugular chain, level IV are located in the lower internal chain and level V are located in the posterior triangle of the neck. Furthermore the central neck (level VI) needs to be evaluated.

**Figure 19** **Level VI contains the thyroid gland, and adjacent nodes, bordered superiorly by the hyoid bone, inferiorly by the brachiocephalic artery, and laterally on each side by the carotid arteries. The level II, III and IV nodes are arrayed along the jugular veins on each side, bordered anteromedially by level VI and laterally by the posterior border of the sternocleidomastoid (SCM) muscle. The level III nodes are bounded superiorly by the hyoid bone, and inferiorly by the cricoid cartilage. Levels II and IV are above and below level III respectively. The level I node compartment includes the submental and submandibular nodes, above the hyoid bone, and anterior to the posterior edge of the submandibular gland. Level V nodes are in the posterior triangle, lateral to the lateral edge of the SCM muscle. Levels I, II and V can be further divided as noted in the figure.**

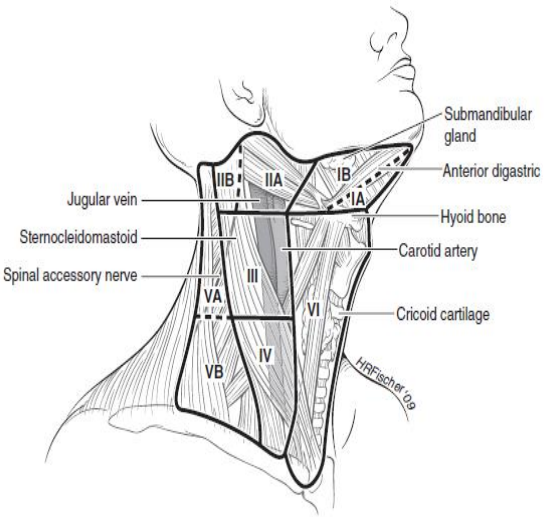


Involvement of lymph nodes with papillary carcinoma may include microcalcifications, cystic changes and focal or diffused increased echogenicity. On color Doppler, pathological lymph nodes may show peripheral flow or chaotic internal vascular pattern [Figures 20-23] [(23)].

According to the guidelines of the American thyroid association, US-guided FNA of sonographically suspicious lymph nodes that are larger or equal to 8-10 mm in the smallest diameter should be performed to confirm malignancy if this would change management.

**Table 3 Sonographic features for the characterisation of malignant and benign nodules.**

| Ultrasound feature | Malignant | Benign |
|---|---|---|
| Solid | ++++ | ++ |
| Mixed | ++ | +++ |
| Purely cystic, thin septa | + | ++++ |
| Hypoechogenic | +++ | +++ |
| Isoechogenic | ++ | +++ |
| Hyperechogenic | + | ++++ |
| Thick incomplete halo | +++ | + |
| Thin halo | ++ | ++++ |
| Poorly-defined margins | +++ | ++ |
| Well-defined margins | ++ | +++ |
| Microcalcifications | ++++ | ++ |
| Eggshell calcifications | + | ++++ |
| Coarse calcifications | + | +++ |
| Internal flow pattern | +++ | ++ |
| Peripheral flow pattern | ++ | +++ |

+, very low probability; ++, low probability; +++, intermediate probability; ++++, high probability

**Figure 20** **Papillary carcinoma, metastatic to cervical lymph nodes in a young male. An anechoic cystic lymph node is shown in the lateral neck, level V. FNA was performed, cytology was positive for papillary carcinoma.**

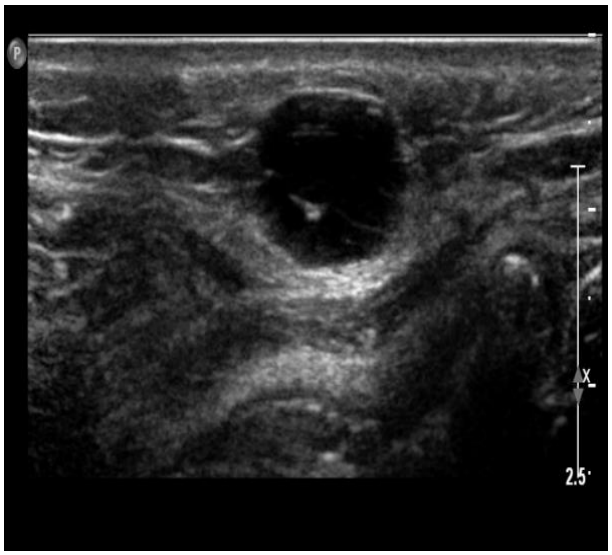


**Figure 21** **Papillary carcinoma metastatic to cervical lymph nodes in a 34-year-old female with a palpable nodule in the right lobe. A mixed cystic and solid nodule with microcalcifications is seen on transverse view (a, b) and longitudinal (c) view of the thyroid gland. Transverse scan of lymph nodes at the jugular chain level III (d). Round small lymph nodes with microcalcifications and without echogenic hilus are seen. Papillary carcinoma was diagnosed on fine-needle aspiration performed from the thyroid nodule and one of the cervical lymph nodes.**

a

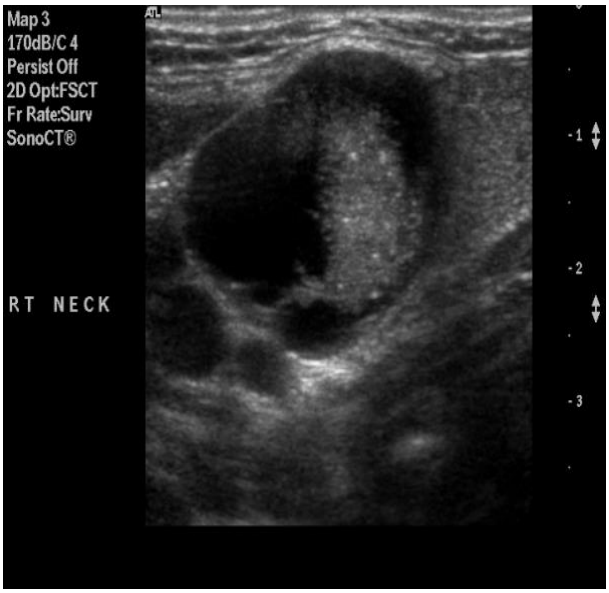
Map 3
170dB/C 4
Persist Off
2D Opt:FSCT
Fr Rate:Surv
SonoCT®
RT NECK

b

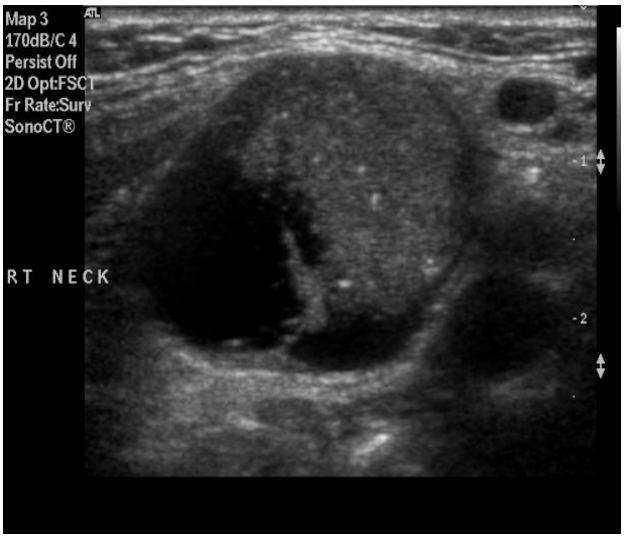
Map 3
170dB/C 4
Persist Off
2D Opt:FSCT
Fr Rate:Surv
SonoCT®
RT NECK

c

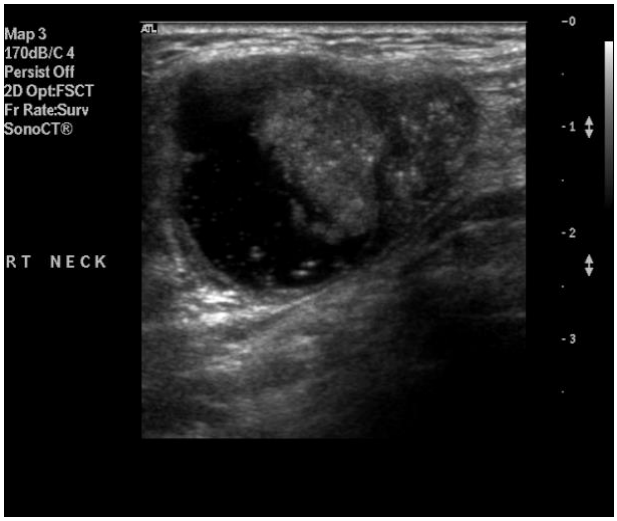
Map 3
170dB/C 4
Persist Off
2D Opt:FSCT
Fr Rate:Surv
SonoCT®
RT NECK

d

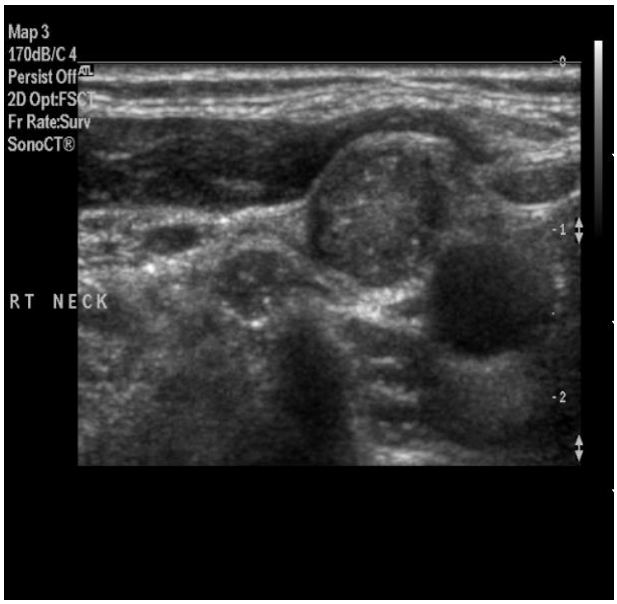


**Figure 22** **Palpable diffusely enlarged thyroid gland in an 18-year-old female. Enlarged right lobe and isthmus (a). Enlarged left lobe (b). Microcalcifications are spread over the whole gland. Distorted vessels on colour Doppler imaging (c). Supraclavicular, level IV, enlarged lymph node with microcalcifications (d). Papillary carcinoma was diagnosed on fine-needle aspiration.**

a

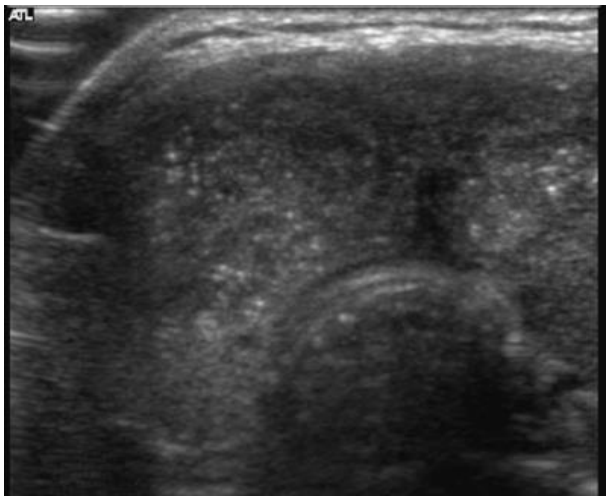

b

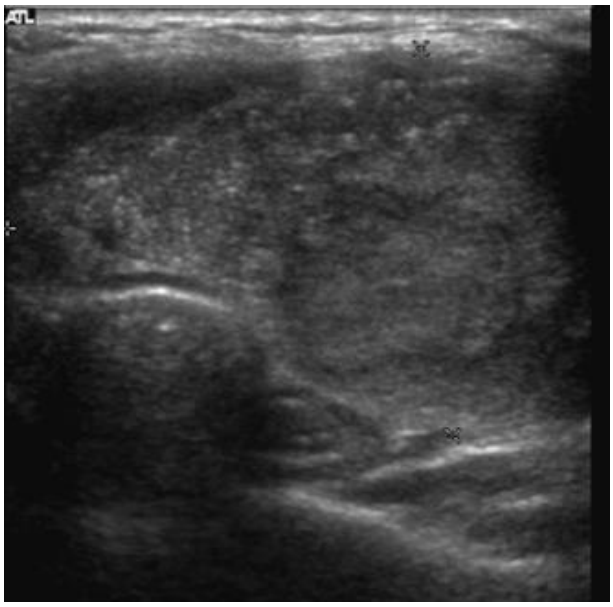

c

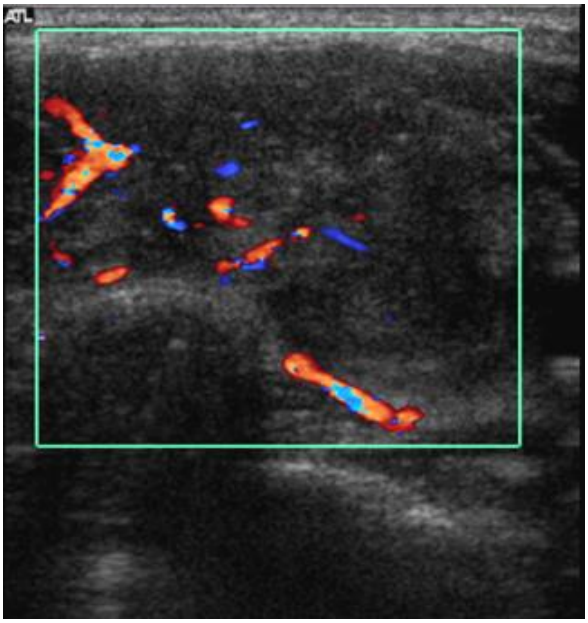

d

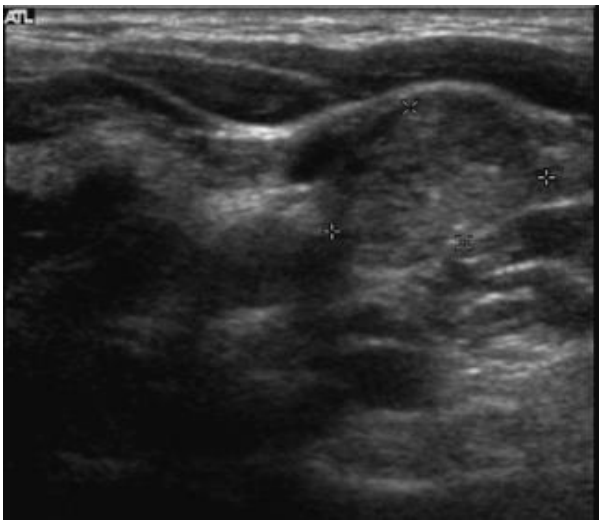

**Figure 23 Papillary carcinoma, metastatic to a lymph node in level II in the right lateral neck. The lymph node is shown with increased echogenicity.**


In one-third of cases, multiple nodules coexist with a malignant nodule. In two-thirds of cases, at least one additional nodule is seen. The “dominant” nodule is the one with features suggestive of malignancy or is different from the other nodules. In 20% of cases papillary carcinoma may be multicentric [Figure 22-23]. In 48% of cases papillary carcinoma may be occult (non-palpable). There is no evidence of a better outcome when an occult carcinoma (under 1–1.5cm) is detected.

Thyroid carcinoma may develop in chronic autoimmune lymphocytic thyroiditis (Hashimoto's thyroiditis) where benign and malignant nodules may coexist. The dominant nodule greater than 1cm in diameter must have a FNA biopsy to rule out carcinoma [Figure 24].

**Figure 24 Palpable nodule at isthmus in a 40-year-old female with hypothyroidism. Multiple tiny hypoechoic nodules spread in the thyroid gland are seen in transverse (a) and longitudinal (b) scans, compatible with Hashimoto's thyroiditis. A 6mm hypoechoic nodule is seen in the isthmus (cursors) in transverse (c) and longitudinal (d) scans through the palpable nodule. Papillary carcinoma was diagnosed on ultrasound-guided fine-needle aspiration (small arrow) of this nodule (e).**

a

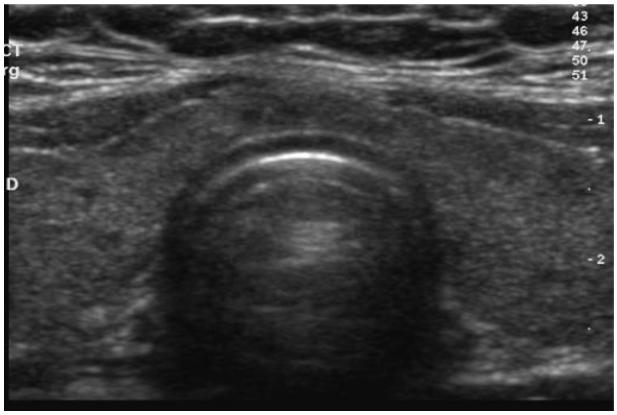

b

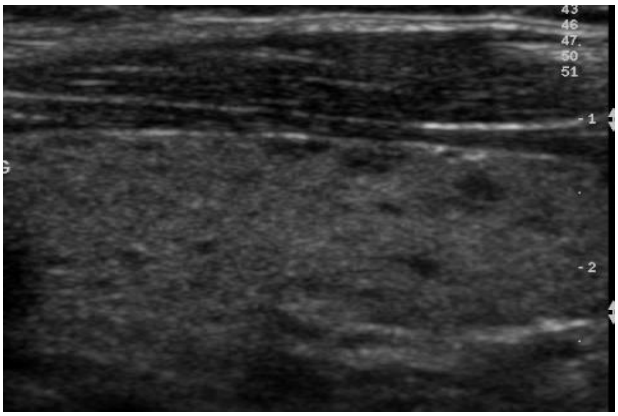

c

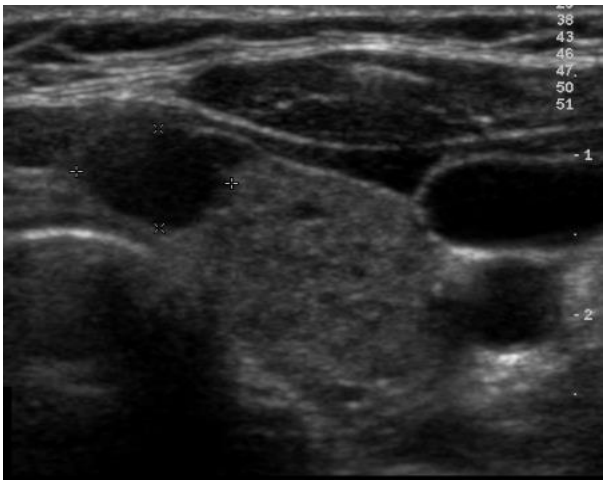

d

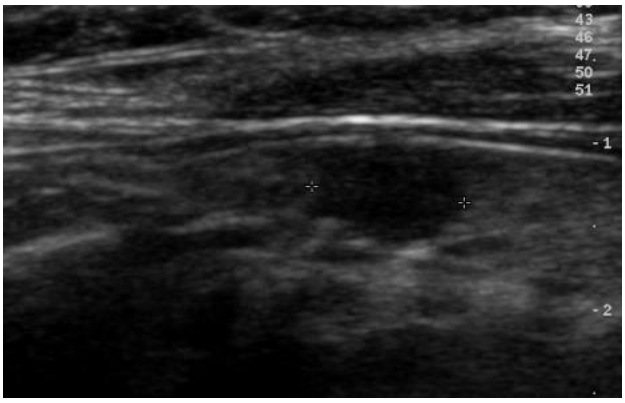

e

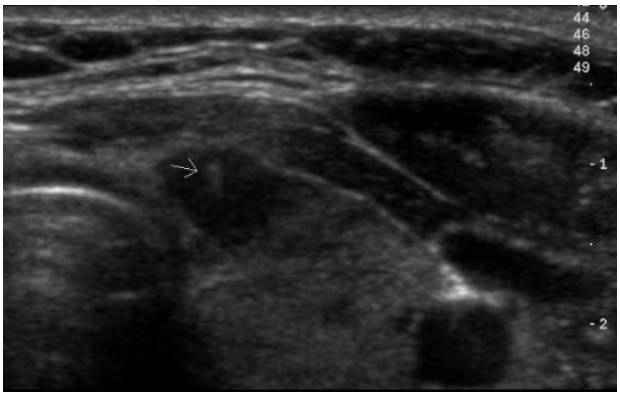

**Follicular carcinoma**

Follicular carcinoma represents 5–15% of all thyroid cancers. Like papillary, follicular carcinoma is more common in females. Two types have been described: minimally invasive type, encapsulated and only invasive to capsular vessels; and widely invasive type, non-

encapsulated and invasive to adjacent tissues and vessels. Metastatic spread to bones, lung, brain and liver may occur with a 5–10% frequency of cases in the minimally invasive type and 20–40% in the widely invasive type. The overall mortality at 20 years is in the range of 20–30%.

Follicular carcinoma is similar to follicular adenoma on sonographic examination. However, the presence of irregular margins, a thick irregular halo and chaotic vessels are suggestive of follicular carcinoma. FNA fails to distinguish between benign and malignant follicular tumours. A follicular “adenoma” must be excised for a definitive diagnosis on histological analysis [Figures 25 and 26].

**Figure 25** **Follicular adenoma in a 42-year-old male. A single nodule was seen in the right lobe. On colour Doppler imaging peripheral to central vessels with a “spoke-and-wheel” appearance can be seen. On fine-needle aspiration a follicular adenoma was diagnosed, although owing to the inability of cytology to differentiate between follicular adenoma and carcinoma, surgery was still performed. Histological analysis confirmed the diagnosis of adenoma.**

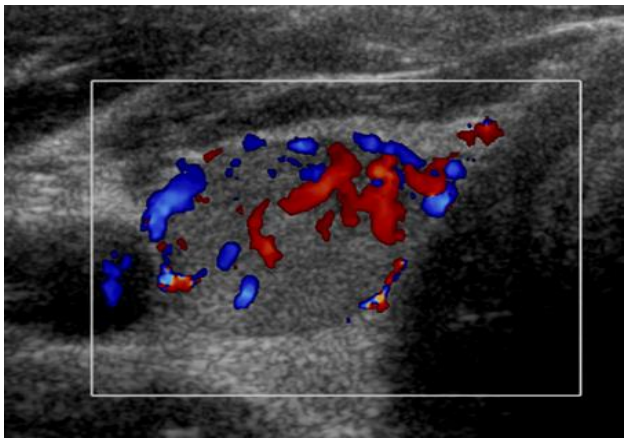

**Figure 26** **Follicular carcinoma. Non-palpable incidentally discovered solitary thyroid nodule in a 56-year-old female during carotid sonography. A bilobular hypoechoic nodule with coarse calcifications (arrow) is seen in the left lobe (a). Disorganised hypervascular network on power Doppler imaging in transverse (b) and longitudinal (c) scans. Fine-needle aspiration was performed yielding a**

**diagnosis of follicular tumour. Partial thyroidectomy was performed, although owing to the presence of sparse malignant cells on histology a total thyroidectomy was performed.**

a

b

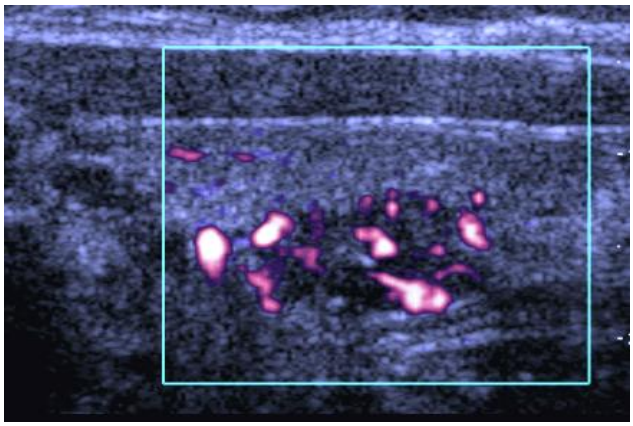

c

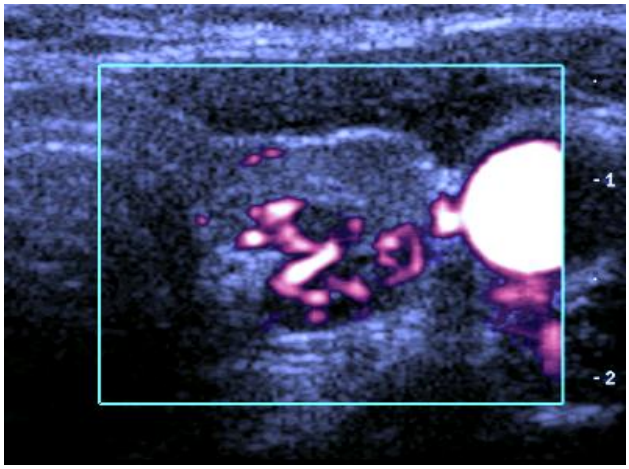

**Medullary carcinoma**

Medullary carcinoma of the thyroid represents 5% of all malignancies. A familial history of thyroid cancer, especially associated with MEN Type II is present in 20%. Medullary carcinoma may secrete calcitonin and frequently spreads to lymph nodes. The prognosis is worse compared with follicular neoplasms. A hypo echoic mass is seen on ultrasound [Figure 27]. Micro calcification may be present, which is coarser than in papillary carcinoma.

**Figure 27 Medullary carcinoma of thyroid in a 38-year-old female. A solitary highly hypo echoic well-delineated oval nodule is seen in the left lobe (a). Sparse peripheral and central vascularisation is seen on colour Doppler imaging (b). Medullary carcinoma was diagnosed on ultrasound-guided fine-needle aspiration (c).**

a

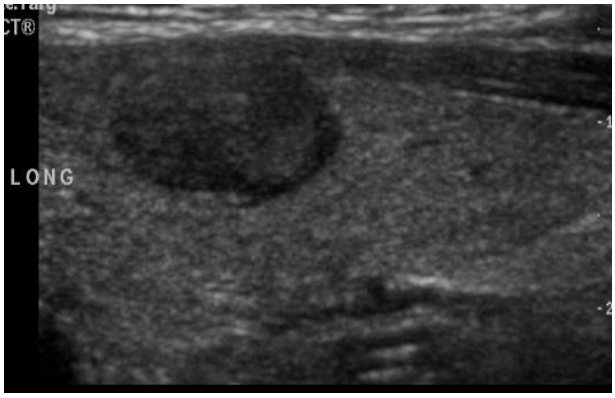


b

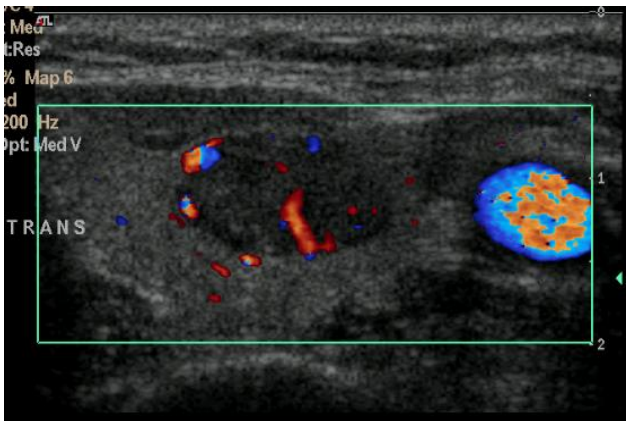


c

**Anaplastic carcinoma**

Anaplastic carcinoma represents 2% of thyroid cancers and is mostly seen in elderly patients. It has the poorest prognosis of all thyroid malignancies with a less than 5% survival rate at five years. Sonographically, the tumour is hypoechogenic, ill-defined and, in general, invasive to adjacent structures [Figure 28].

**Figure 28 Anaplastic carcinoma of the thyroid in an 86-year-old female. Transverse scan (a). Longitudinal scan (b). A large hypoechoic undefined tumour invading the adjacent muscles is seen in the right lobe. Ultrasound-guided needle biopsy with an 18-G Tru-cut needle (echogenic line into the nodule) was performed because of suspicion of a lymphoma (c). The histological diagnosis was anaplastic carcinoma of the thyroid gland.**

a

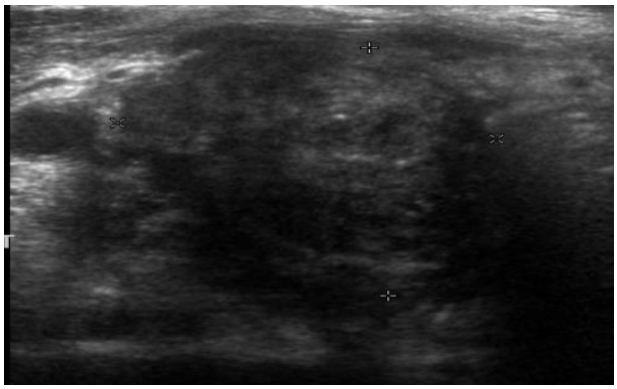

b

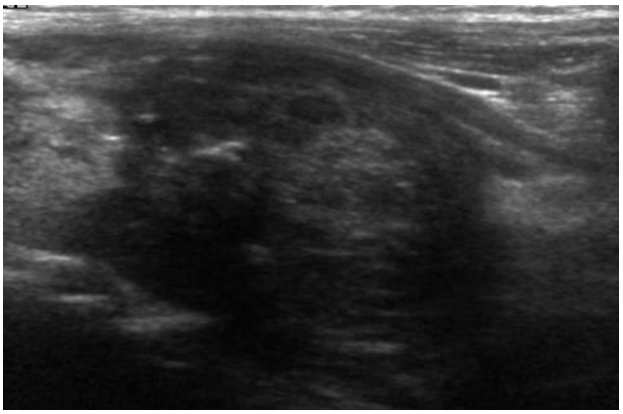

c

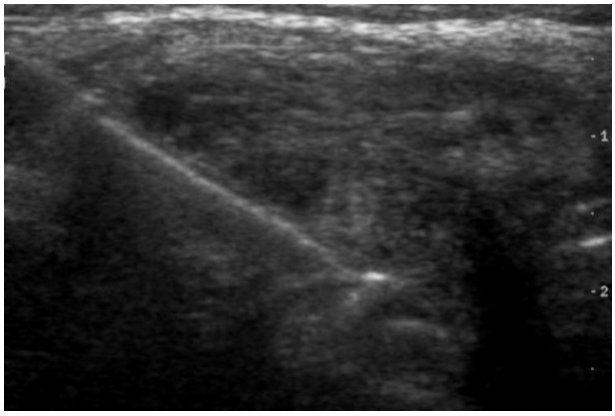

**Thyroid lymphoma**

Thyroid lymphoma represents 4% of all malignancies of the thyroid. Histologically, it is a non-Hodgkin's type. Patients are mostly elderly women; 60–70% develop on the basis of a chronic lymphatic thyroiditis. It grows rapidly and surveillance depends on the clinical stage. It can appear as one or more markedly hypoechoic lobulated masses [Figure 29], sometimes with cystic necrosis. On colour Doppler they are hypovascular with chaotic vessels. Neck vessels encasement may be seen.

**Figure 29 Thyroid lymphoma in a 43-year-old female with non-Hodgkin's lymphoma. Thyroid nodules were seen on neck CT. Multiple hypoechoic nodules seen on transverse and longitudinal scans (a, b). Fine-needle aspiration under**

**ultrasound guidance from the dominant nodule in the left lobe (arrow) rendered non-Hodgkin's lymphoma (c).**

a

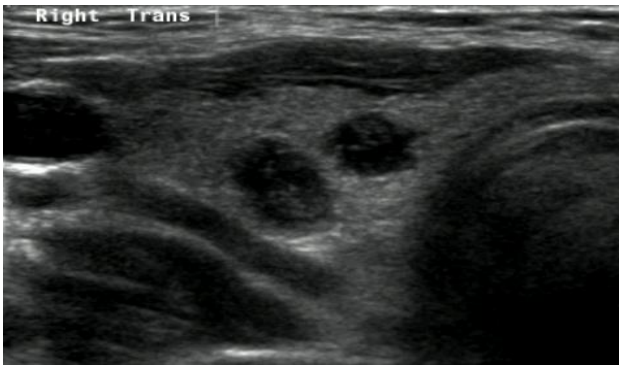


b

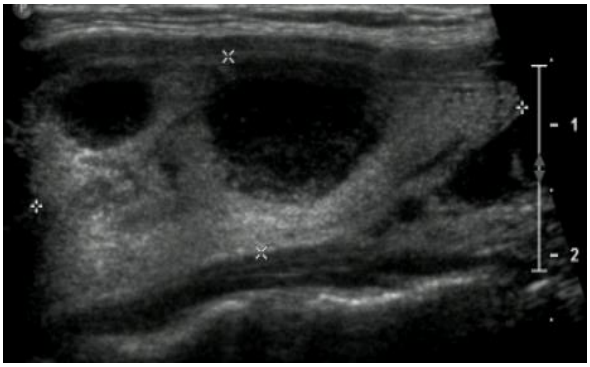


c

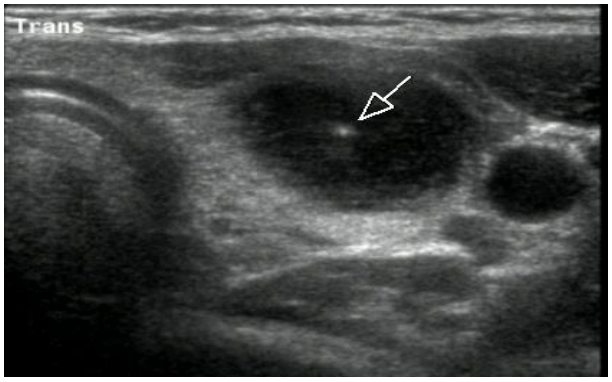


## Thyroid metastases

Metastases to the thyroid gland are infrequent and generally associated with an advanced stage of malignancy. The main primary tumours that spread to the thyroid gland are

malignant melanoma (39%), breast carcinoma (21%) and renal cell carcinoma (10%). Sonographically, metastases are present as a solitary or multiple hypo echoic homogeneous mass without calcification [Figures 30 and 31].

**Figure 30 Relapse of squamous cell carcinoma of the oesophagus at the cervical anastomosis, which invades the thyroid gland in a 76-year-old male. On a transverse scan a lobulated highly hypo echoic mass (M) infiltrating the right lobe of the thyroid (T) is seen, common carotid artery (CCA); jugular vein (JV) (a). On a longitudinal scan the mass (M) infiltrates the lower pole of the thyroid (T) (b).**

a

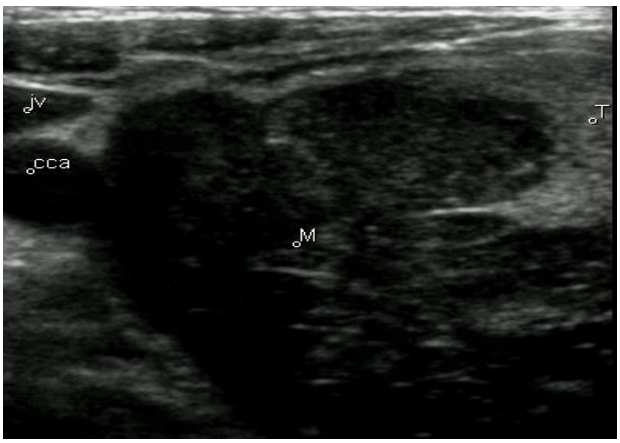


b

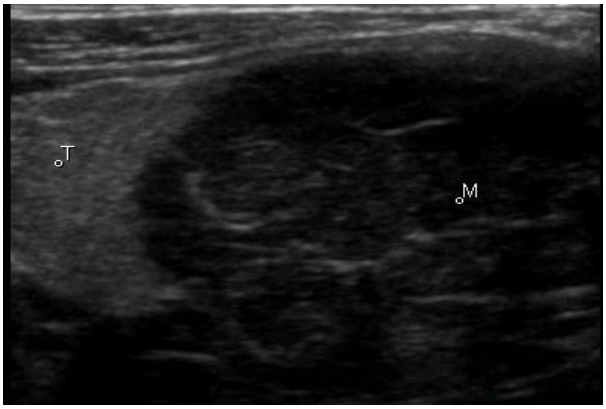

**Figure 31 Metastases from gastrointestinal adenocarcinoma. Bilateral thyroid nodules are seen in a CT scan in a 55-year-old female with a suspected malignancy of unknown origin. Transverse scan of the right thyroid lobe shows several small hypo echoic nodules (a). Transverse scan of the left lobe showing a big hypo echoic nodule (b). Adenocarcinoma most probably of gastrointestinal origin was diagnosed on fine-needle aspiration.**

a

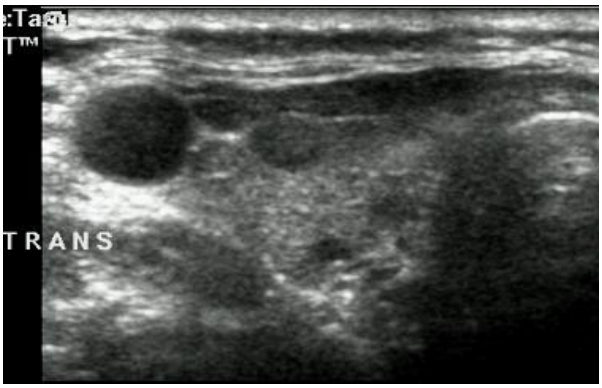


b


## Monitoring after thyroidectomy

Two techniques are recommended for monitoring of malignancy post-thyroidectomy: $I^{131}$ whole-body scanning and/or thyroid sonography imaging and measurement of serum

thyroglobulin. Suggested surveillance and a maintenance protocol for DTC (papillary and follicular types) include periodic neck ultrasonography and chest radiography [Figure 32].

**Figure 32 Recurrent papillary carcinoma in the thyroid bed. A young female, several years after total thyroidectomy due to papillary carcinoma. A 3.5 cm ill- defined mass is shown in the right thyroid bed (arrow). The mass is hypoechoic with microcalcifications. FNA was performed, cytology was positive for papillary carcinoma.**

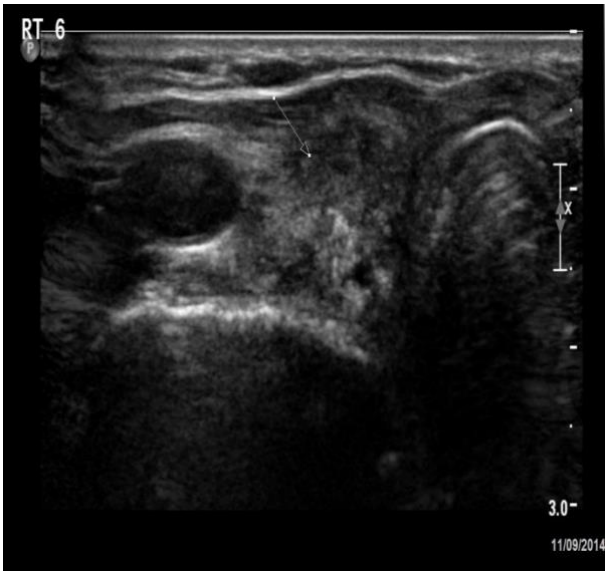


Ultrasonography performed by an experienced operator is the most sensitive means for detecting neck recurrence of DTC [(24)].

***Monitoring after thyroidectomy- role of ultrasound***

According to the guidelines of the American thyroid association, cervical ultrasound, to evaluate the thyroid bed and the central and lateral cervical nodal compartments, should be performed 6-12 months following surgery and then periodically according to the patient's risk for recurrent disease and thyroglobulin status.

If a positive result would change management, sonographically suspicious lymph nodes ≥8-10 mm (see above) in the smallest diameter should be biopsied. Suspicious lymph nodes

smaller than 8-10 mm in the smallest diameter may be followed up without biopsy. If growth of the lymph node is seen, or the node threatens vital structures FNA should be considered. Cervical Ultrasound should examine all lymph node compartments including the thyroid bed [Figure 33].

**Figure 33 Recurrent papillary carcinoma in thyroid bed with a retrojugular lymph node metastasis in a 48-year-old female under surveillance following thyroidectomy. Non-palpable 6mm width (cursors) hypoechogenic and ill-defined nodule (arrow) with microcalcifications (open arrow) at isthmus bed (a). Retrojugular round lymph node (arrows) with microcalcifications (b). Ultrasound-guided fine-needle aspiration (small arrow) from the lymph node yielded the diagnosis of relapsing papillary carcinoma (c). JV, jugular vein; CA, carotid artery.**

a

b

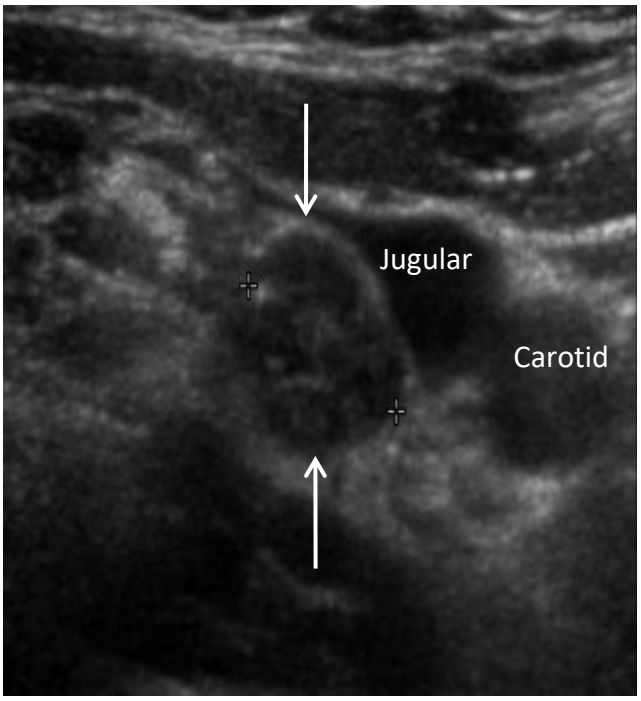


c

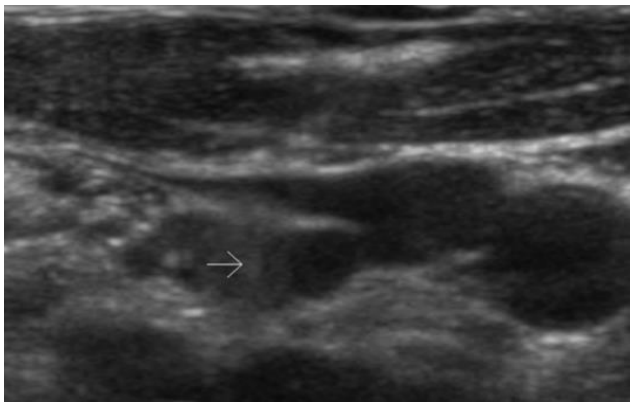

A comparison of US findings and pathology at time of surgery [(25)] has shown that for lymph nodes >7 mm in the smallest diameter, a cystic appearance or hyperechoic punctuations on ultrasound should be considered malignant. Furthermore this comparison has shown that lymph nodes with an hyperechoic hilum are reassuring but a round shape, a hypoechoic appearance or loss of an hyperechoic hilum by themselves do not justify biopsy. Kim DW and colleagues found that the sonographic features of metastatic cervical lymph nodes in postoperative patients with papillary thyroid carcinoma were similar to those in preoperative patients [(26). Interpretation of neck US should take into account all clinical and laboratory data. The risk of recurrence is related to the initial lymph node involvements

most recurrences are seen in already involved compartments [(27)]. In low and intermediate risk patients; the risk of lymph node recurrence is low (<2%) when serum thyreoglobulin (Tg) Level is undetectable [(28)].

**Fine-needle aspiration cytology**

Cytological examination of material obtained by FNA is the best single test for differentiating malignant from benign thyroid lesions owing to its high sensitivity and specificity. FNA was first used in Sweden in the 1950s, but it did come in to wide use until the 1980s. FNA is performed under ultrasound guidance using 21–27-G needles. In the fine needle cytology classic approach, the biological specimen is obtained by repetitively moving a needle attached to a 10–20ml syringe for constant or intermittent suction. A more recent variation is to collect the specimen by moving through and twirling a small needle within the nodule, which is not attached to a syringe, to aspirate the material by capillary action. The material is air-dried, stained with Papanicolaou and May-Grünwald-Giemsa or haematoxylin and eosin and interpreted by a cytopathologist. Ultrasound imaging guidance enables the introduction of the needle into the core of the lesion in real-time, thus considerably improving diagnostic accuracy and sensitivity compared with blind aspirations [(29)]. In our experience, 22-G needles provide excellent results without major complications. Bleeding occurs in 1% of aspirations and is usually self-limiting. The practice of thyroid FNA cytology varies in different countries and institutions. In most institutions, samples are taken by cytologists, cytopathologists or cytotechnologists, while radiologists position the needle within the lesion under ultrasound-guidance. The needle should be continuously monitored by the ultrasound beam during the procedure. Therefore, we recommend the insertion of the needle from the edge of the transducer and not in the middle. By inserting the needle from the edge, it is possible to visualise the whole length of the shaft of the needle during the whole procedure, and to be sure that the needle tip is in the desired position. If the needle is inserted in the midline of the transducer, the tip of the needle might not be accurately visualised during the procedure [Figure 34].

**Figure 34 The needle is introduced from the side of the linear transducer and its whole length is clearly visible (arrows) within the nodule during the procedure.**

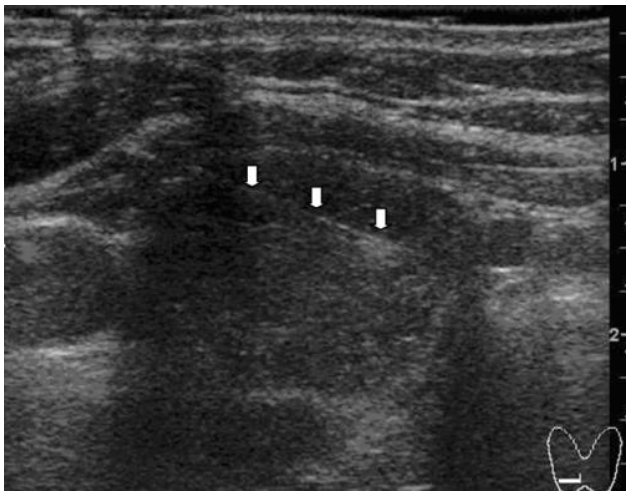

**TIRADS -Thyroid imaging reporting and Data System for US features of nodules**

Although many reports have demonstrated malignant ultrasound features necessitating US-guided fine needle aspiration biopsy (FNAB), it was still difficult to decide which nodule to aspirate due to different guidelines and classifications [(6)]. In 2005 M.C Frates et al published a consensus regarding management of thyroid nodules detected by Ultrasound [(30)] [Table 4].

**Table 4 Recommendations for work-up of thyroid nodules 1 cm or larger in maximum diameter.**

| US Feature | Recommendation |
|---|---|
| Solitary nodule | |
| Microcalcifications | Strongly consider US-guided FNA if ≥ 1 cm |
| Solid (or almost entirely solid) or coarse calcifications | Strongly consider US-guided FNA if ≥ 1,5 cm |
| Mixed solid and cystic or almost entirely cystic with solid mural component | Consider US-guided FNA if ≥ 2 cm |

| | |
|---|---|
| None of the above but substantial growth since prior US examination | Consider US-guided FNA |
| Almost entirely cystic and none of the above and no substantial growth (or no prior US) | US-guided FNA probably unnecessary |
| | |
| Multiple nodules | Consider US-guided FNA of one or more nodules, with selection prioritized on basis of criteria (in order listed) for solitary nodule* |

In 2009, Park JY et al. [(31)] and Horvath E et al. [(32)] published two studies suggesting a reporting data system for thyroid lesions to stratify the risk of malignancy in nodules. These two classification systems were based on the Breast Imaging Reporting and Data System (BI-RADS), which was developed by the American College of Radiology [(33)] and were named TIRADS - Thyroid Imaging Reporting and Data System. However, the data system that they developed was found to be difficult to apply in the clinical setting due to their complexity. Kwak JY et al. [(6)] aimed to develop a practical TIRADS with which to categorize thyroid nodules and stratify their malignant risk. Their study included nodules that were at least 1 cm. In their study the following US features were found to be significantly associated with thyroid cancer: solid component, hypoechogenicity (compared to thyroid parenchyma), marked hypoechogenicity (less than the surrounding strap muscles), microlobulated or irregular margins, microcalcifications and taller - than - wide shape. Multivariate analysis showed that the risk of malignancy increases as the number of suspicious US features increases.

With these findings, Kwak JY et al. described TIRADS categories are as follows:

- TIRADS 3- no suspicious US findings- safe to follow up [Figure 35]
- TIRADS 4a- one suspicious US feature - FNAB indicated [Figure 36]
- TIRADS 4b- two suspicious US features- FNAB indicated [Figure 37]
- TIRADS 4c- three or four suspicious US features- FNAB indicated
- TIRADS 5- five suspicious US features- FNAB indicated [Figure 38]

**Figure 35** **A cystic nodule (calipers), with a "ring down" or "comet tail" artifact. No malignant features. TIRADS 3 (according to Kwak et al.), TIRADS 2 (according to Horvath et al.) or TIRADS 1 (according to ACR) all designating the nodule as benign. FNAB not indicated.**


**Figure 36** **A solid echogenic nodule (arrow). Showing one malignant feature - TIRADS 4a (according to Kwak) indicating FNAB, or TIRADS 3 (according to ACR) indicating FNAB when nodule is equal to or larger than 2.5 cm. FNAB performed and cytology was benign.**

**Figure 37 A solid hyopechogenic nodule (arrow), undefined margins. Showing two malignant features TIRADS 4b (according to Kwak) indicating FNAB or TIRADS 5 (according to ACR) indicating FNAB only when nodule is equal to or larger than 1 cm. Papillary carcinoma on cytology.**

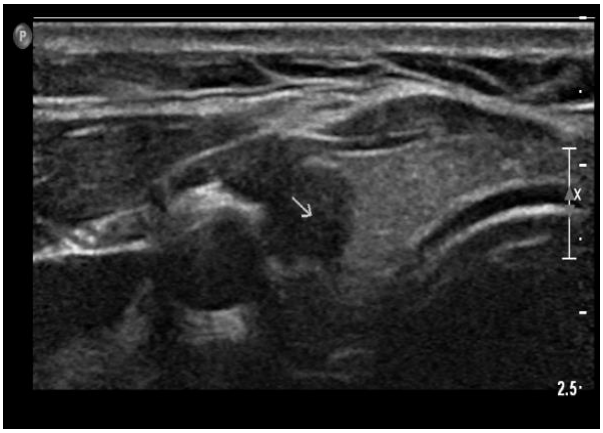

**Figure 38 A solid, hypoechogenic nodule (arrow). Margins are undefined, taller than it is wide and microcalcification are shown within the nodule. TIRADS 5 according to both Kwak and ACR. FNAB indicated. Papillary carcinoma on cytology.**

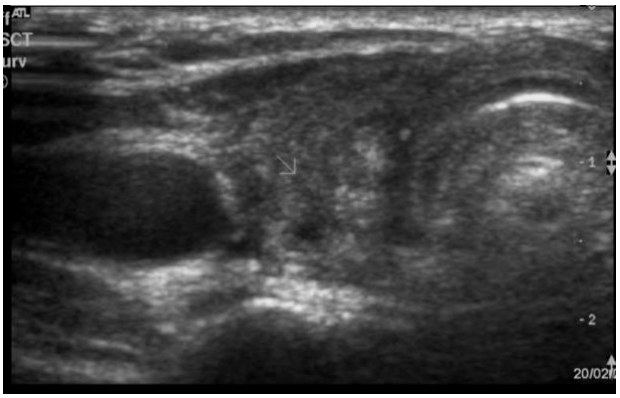

Horvath et al. [(32)], specified 10 different US patterns including TIRADS 2 that includes 3 types of colloid nodules; anechoic cyst (colloid 1), spongiform nodule- grid like appearance (colloid 2) and mixed with solid portion (colloid 3) all of which are defined as having no risk of malignancy. The description of the latter type (colloid 3) actually contradicts Kwak et al.

[(6)] that designated any solid portion as a feature found to be significantly associated with thyroid cancer.

In 2017 the ACR committee published their recommendations to provide guidance regarding management of thyroid nodules on the basis of their ultrasound appearance [(2)], ranging from TIRADS 1 to TIRADS 5 according to 5 groups of criteria, as well as supplying recommendations for follow up or FNA. We need to emphasize that no single thyroid imaging reporting system has been agreed upon for universal application. However, the authors of this chapter find the ACR guidelines most efficient and simple to use.

**The Bethesda System for Reporting Thyroid Cytopathology**

FNAB has been proven efficient, accurate, inexpensive and safe for the differential diagnosis of thyroid nodules, but still has inherent diagnostic limitations such as non-diagnostic, inadequate or unsatisfactory results. The criteria used to determine specimen adequacy vary among cytopathologists, leading to confusion in patient treatment. The Bethesda System for Reporting Thyroid Cytopathology [(34-38)] was introduced in 2009 and reviewed in 2017 to help overcome this inconsistency and provide cytologic reports with uniform terminology among pathologists and laboratories and improve communication between pathologists, clinicians, surgeons and radiologists. Yoon JH et al. found in a recent study that nodules with non-diagnostic results of evaluation with the Bethesda System that are assessed as TIRADS (Kwak) [(6)] category 3 or 4a may be managed conservatively with follow up [(39)]. Both the ATA guidelines and the TIRADS ACR provides criteria for risk assessment of thyroid nodules. Certain sonographic features have been frequently associated with malignancy. These include microcalcification, taller than wide shape and extrathyroidal extension. When examining the ATA criteria it is seen that echogenic or isoechoic nodules with one or more of these features cannot be categorized based on the ATA guidelines. Gao L et al. found 70/2614 (2.7%) "unspecified" nodules. 18.6% of these nodules were malignant, when using the ATA guidelines [(40)]. Middelton et al. [(41)] found 477/3422 (13.9%) "unclassified" nodules, 12.8 % of these nodules, were malignant when using the ATA guidelines [(41)]. In a study we are now conducting 10/198 nodules could not be graded according to ATA. From these none were proven to be malignant by cytology however this is a very small cohort compared to the Middleton study.

## Diffuse disease

There are several conditions that can be thought of as causing a diffuse abnormality within the thyroid. This section will deal with only the most common of these namely MNG, Hashimoto's thyroiditis, De Quervain's subacute thyroiditis and Graves' disease. Many of these processes will have similar ultrasound characteristics, but have widely differing clinical presentations. For example, Hashimoto's thyroiditis and Graves' disease can look very similar on ultrasound yet clearly have widely differing biochemical profiles and clinical presentations. The operator needs to be aware that the ultrasound findings should not be viewed in isolation from the clinical and biochemical status of the patient. Ultrasound has no primary role in the management of the hyper- or hypothyroid patient; biochemistry is the mainstay in determining management. However,the ultrasound operator should be aware of the clinical features of these conditions because many diffuse diseases of the thyroid will present as a "thyroid nodule".

### Multinodular goiter (MNG)

MNG is the commonest pathological condition of the thyroid. The ultrasound diagnosis rests on the identification of multiple nodules within an enlarged thyroid. The features that indicate that the nodules are benign are the same as those described in the previous section. To understand the ultrasound morphology one needs to review the basic pathological processes of the development of MNG. Hyperplasia occurs with the subsequent formation of nodules. There is associated fibrosis and calcification within the nodules. Vascular compression due to follicular hyperplasia leads to focal ischaemia, necrosis and inflammatory change. Cystic areas contain colloid, identified microscopically, alternate with hyperplastic foci of thyroid tissue. There is haemorrhage, fibrosis and calcification. Secondary to the inflammatory changes, a lymphocyte infiltration may be found [(9)]. In light of these histological changes, the ultrasound features of the development of MNG [Figure 39] are:

1. iso- or hyperechoic nodules with cystic degeneration;
2. well-defined halo surrounding nodules due to compressed adjacent tissue;
3. colloid component of cystic elements, "ring down" sign;
4. heterogeneous background echo-texture of the thyroid; and

5. calcification nodules often contain florid dysplastic central calcification or well-defined peripheral curvilinear calcification.

**Figure 39 Multinodular goiter. Diffuse parenchymal inhomogeneity over the two lobes and the isthmus. They were imaged separately owing to their large size and afterwards joined to show the whole gland, without any recognisable normal tissue.**

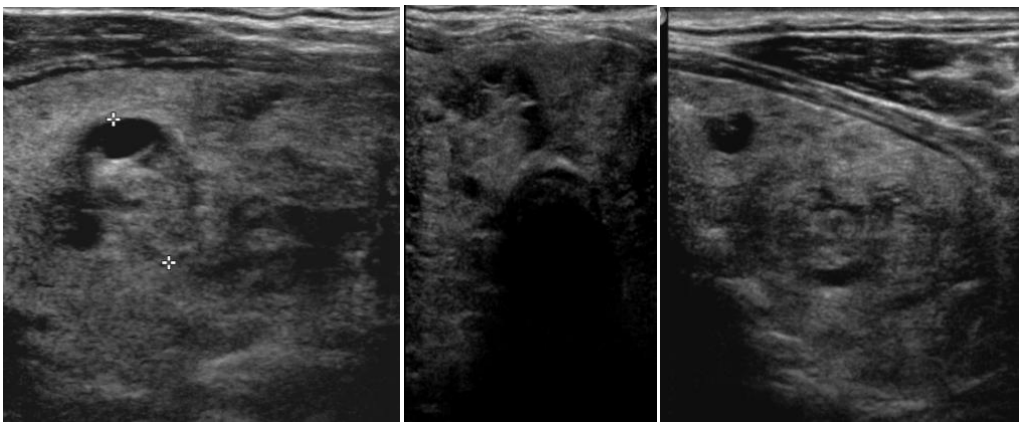

Frequently the only role for ultrasound in the management of MNG is to confirm the clinical diagnosis. The radiologist or sonographer can add value to the examination by assessing the nodules to ascertain whether there are any features to suggest that there may be a malignant nodule within. If no features are present, biopsy or FNA is of little value in the confirmation of a MNG and should be discouraged. An assessment of retrosternal extension should be carried out as part of the examination by scanning inferiorly to the level of the manubrium and, if necessary, asking the patient to swallow to identify the lower margin of the thyroid. If retrosternal extension is detected, CT is required to define the mediastinal extent.

**Thyroiditis**

The most common forms of thyroiditis encountered are Hashimoto's thyroiditis and De Quervain's thyroiditis. This section will discuss these plus Graves' disease.

### *Hashimoto's thyroiditis*

Hashimoto's thyroiditis is the most common of the chronic thyroiditides and the commonest cause of hypothyroidism. It is an autoimmune condition. Hypothyroidism is diagnosed at presentation or develops subsequently in 50% of cases. Biochemically, hyperthyroidism is seen in the acute initial phase.

*Ultrasound appearances*

*Acute phase*

Focal nodular thyroiditis demonstrates small hypoechoic nodules with ill-defined margins, which represents lymphocyte infiltration [Figure 40]. Features typically start in the anterior portion and isthmus of the thyroid.

**Figure 40 Early Hashimoto's thyroiditis. Note the hypoechoic changes commence in isthmus and anterior portion of right lobe of the thyroid.**

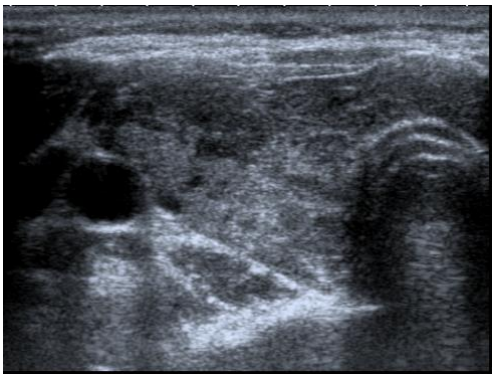

*Sub-acute phase*

Infiltration continues to involve the whole of the thyroid gland. The gland is enlarged and has a slightly rounded outline. It can be hypervascular on colour flow imaging [(4, 42, 43)].

*Chronic phase*

Enlarged, slightly lobular outline is seen. The thyroid is diffusely hypoechoic with fine echogenic septae within [Figure 41]. The atrophic gland is small with heterogeneous echogenicity.

**Figure 41 Established Hashimoto's thyroiditis. Note echogenic striae against the hypoechoic background and diffuse changes throughout the gland. (a) Axial scan. (b) Longitudinal scan.**

a

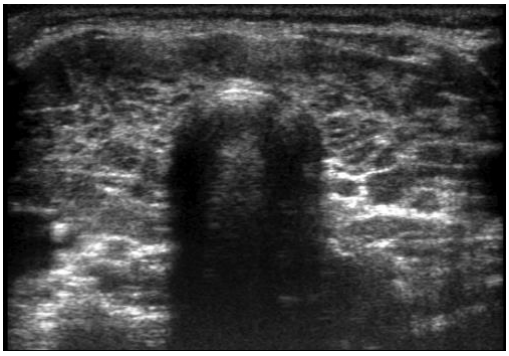

b

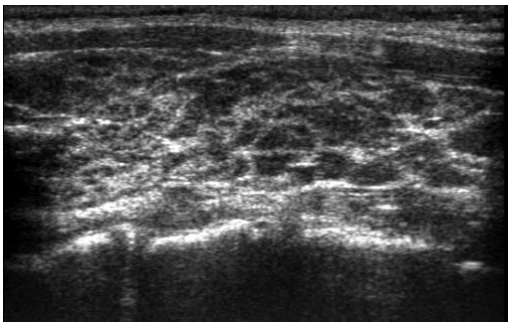

***De Quervain's subacute thyroiditis***

The clinical scenario differs because the patient characteristically presents, typically following a viral illness, with a painful swelling in the lower neck, fever and lethargy. The biochemistry in the acute phase is thyrotoxicity, which is usually followed by a period of hypothyroidism. Typically (after a period of 6 months from acute onset) the patient recovers and becomes euthyroid.

*Ultrasound features*

*Acute phase*

A hypoechoic ill-defined mass, which is usually tender. The adjacent thyroid tissue has a heterogeneous echotexture.

*Subacute phase*

The hypoechoic area increases in size to involve the ipsilateral thyroid lobe and sometimes extends to the contralateral lobe.

*Recovery phase*

Thyroid appearances returns to normal or atrophy may develop.

***Grave's disease***

The typical biochemical thyrotoxic profile is matched by a diffuse enlargement of the thyroid gland with rounding of the normal angular outline. The gland is diffusely hypoechoic and colour flow imaging reveals an often spectacular "thyroid inferno" with marked hypervascularity [Figure 42]. The ultrasound picture can be indistinguishable from Hashimoto's thyroiditis in the sub-acute phase or can be indistinguishable from de Quervain's thyroiditis if both lobes are involved. However, the clinical picture varies significantly between the three conditions, which make an ultrasound distinction between the conditions academic.

**Figure 42 Hypervascularity identified in early Grave's disease. The appearance is non-specific and can be seen in any acute thyroiditis (for example, anterior distribution could be seen in early Hashimoto's thyroiditis).**

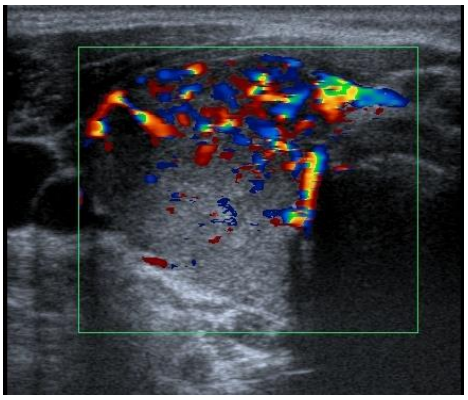

## Percutaneous ultrasound-guided ethanol injection for the treatment of thyroid toxic and autonomous nodules

Thyroid toxic adenomas and toxic nodular goitres have traditionally been treated with radioiodine therapy or surgical resection. According to the numerous literature reports, both methods are associated with potentially serious, permanent and relatively frequent complications [(37)]. Ethanol is a well-established sclerosing agent in the treatment of hepatocellular carcinomas using ultrasound guidance [(32)]. Solbiati et al [(45)] introduced this technique in the neck for sclerosing parathyroid glands in patients with secondary hyperparathyroidism. In 1990, Livraghi et al [(31)] reported the use of ultrasound-guided percutaneous ethanol injection (PEI) for sclerosing autonomous and toxic thyroid adenomas. Mostly single autonomous and toxic adenomas are treated and the results for the treatment of toxic nodular goitre are poor. The PEI procedure is performed in two sessions per week until the total calculated volume is injected. PEI is performed under ultrasound guidance using state-of-the-art scanners *i.e.* colour and power Doppler ultrasound, to evaluate increased intra- and perinodular vascularisation, which can be observed in the vast majority of autonomous (scintigraphically "hot") thyroid nodules [Figure 43].

**Figure 43 Colour Doppler imaging demonstrates hypervascularisation of thyroid toxic adenoma before treatment.**

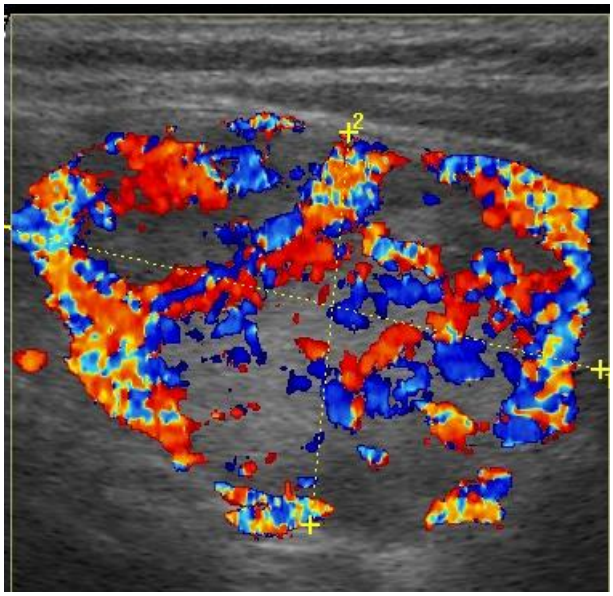

The needle is introduced into the nodule using a “free-hand” technique without the use of local anesthaesia. Side-hole needles are preferable, although end-hole needles are suitable too. Sterile 96% ethanol is used as the sclerosing agent. The total volume of ethanol should equal 1.5 times the nodular volume. The nodular volume (in cubic centimetres) is calculated by:

length × width × depth × 0.5 = volume in $cm^3$

The number of injections (or sessions) is calculated according to the nodule size and usually varies from one to eight injections for the therapy cycle. The volume of ethanol being injected per session depends on patient compliance; in large nodules it is up to 30% of the nodular volume, while in small nodules the total ethanol volume can be injected in 1 or 2 sessions. At each session ethanol is injected with the needle directed at different areas of the nodule to ensure equal distribution. The procedure is repeated twice a week until the calculated volume of ethanol has been injected into the nodule. Injection and distribution of ethanol within the nodule is clearly visible as tiny intranodular hyperechoic foci using ultrasound control [Figure 44].

**Figure 44 During ethanol injection, hyperechoic foci are seen within the nodule (arrows). Equal intranodular distribution of ethanol can be achieved by modifying the position of the needle.**

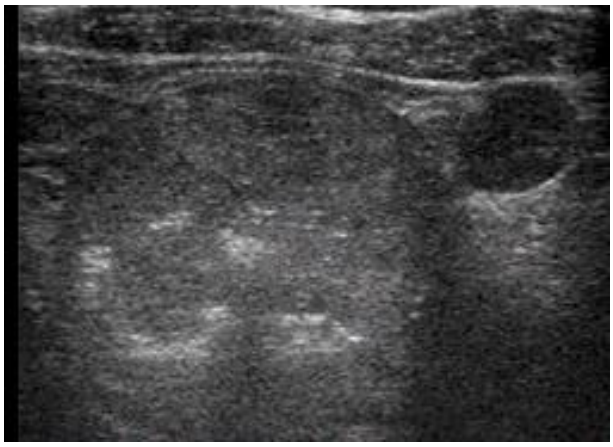

Thyrostatic medication is not routinely prescribed prior to PEI. In all patients, thyroid hormones, thyroid-stimulating hormone (TSH) and thyroid antibodies in the serum are measured using standard laboratory methods and thyroid scintigraphy using $^{99}Tc^{m}$ pertechnetate is performed. Scintigraphic and ultrasound/colour Doppler imaging findings are compared prior to PEI so ethanol can be injected into the specific nodule, which has proved to be particularly beneficial in cases of multinodular thyroids.

Follow-up after PEI includes measurement of serum thyroid hormones and control ultrasound examination at 1, 3, 6 and 12 months. Thyroid scintigraphy is performed 3–4 months after completion of PEI. Evaluation of PEI success is based on hormonal status and scintigraphic findings. If the procedure was not successful upon the first cycle of injections, ethanol can be reinjected once more. If new autonomous nodules develop during the period of follow-up PEI can be repeated.

Possible complications are minor and transitory. Some patients develop local haematoma after the procedure that usually resolves spontaneously. All patients experience pain during the ethanol injection and 30–40% experience pain a few hours to 2 days after the procedure. Pain is usually well-tolerated, but approximately 5% of patients refuse further treatment. Pain is projected towards the jaw, ear or sternum, and is stronger when more ethanol is injected. Transient dysphonia may result after injection of ethanol in posterior parts of the lobe.

The outcome of PEI can be categorised into three groups [(8, 12, 30)]:

1. Complete cure with normalisation of serum thyroid hormones and TSH levels, normalisation of the clinical status and reappearance of the extranodular uptake on scintigraphy, while the node is either “cold” or invisible on the scan.
2. Partial recovery with remission of clinical symptoms, normalisation of serum thyroid hormones and TSH levels, reappearance of the extranodular uptake on scintigraphy with node (or part of the node) still “hot” on scintigraphy.
3. Hormonal remission. Clinical status improved, serum thyroid hormone levels normal, TSH still suppressed and scintigraphically “hot” nodule, with suppressed extranodular uptake.

In our experience, complete cure is achieved in some 60% of patients, partial recovery in 28–30% of patients and failure of the procedure is observed in 10–12%. Both complete cure and partial recovery are considered a successful treatment. The best results are seen for autonomous nodules where some uptake of technetium is seen in extranodal thyroid tissue on scintigraphy. The success rate for toxic nodular goitre is below 50%. In more than 90% of patients we observed significant reduction of the initial nodular volume during the follow-up, with a volume reduction >50% due to coagulation necrosis induced by ethanol and subsequent nodular fibrosis. In all patients with a successful procedure outcome considerable flow reduction or even the disappearance of intranodular flow was observed with colour and power Doppler imaging [Figure 45 and 46]. B-mode echogenicity increased in all successfully sclerosed nodules [(10, 11)].

**Figure 45 2 days after the first percutaneous ethanol injection session the nodule vascularisation is markedly decreased.**

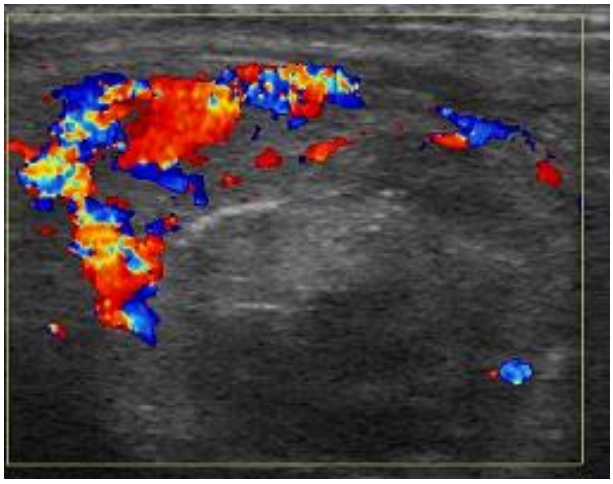

**Figure 46 Power Doppler imaging demonstrates almost completely absent internal vascularisation after successful completion of the procedure.**

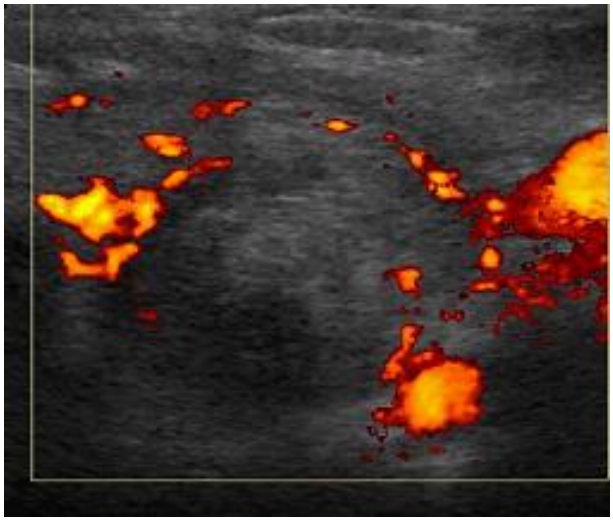

One might speculate whether PEI should only be used in patients with toxic adenomas. Patients with autonomous adenomas rarely disclose clinical symptoms and may undergo spontaneous degeneration, involution and self-healing. However, PEI in developing autonomous adenomas prevents the development of overt hyperthyroidism in the future.

Young female patients with solitary hyperfunctioning nodules are ideal candidates for PEI, especially those with autonomous adenomas. This group of patients should avoid exposure to radioactive isotopes because of long lasting hypothyroidism that follows this particular therapy. Hypothyroidism following PEI is extremely rare (<1%) [(28, 29, 35)]. Unlike PEI, radioiodine therapy causes hypothyroidism in 5–30% of patients and is known to increase the incidence of gastric carcinoma. After thyroid gland surgery, hypothyroidism is observed in 11% of cases. Other serious complications include permanent recurrent laryngeal nerve damage and hypoparathyroidism [(44)]. Both radioiodine therapy and surgery are considerably more expensive compared to PEI.

In conclusion, ultrasound-guided PEI is a safe and effective method for the treatment of autonomous and toxic thyroid nodules. It enables permanent inactivation of autonomous nodules in up to 90% of patients and has minimal and transitory side effects. The best results are observed in patients with small and solitary nodules and it may become the treatment of choice for toxic and autonomous solitary nodules, especially in young patients.

## Other imaging modalities

### Elastography

Elastography is a newly developed sonographic dynamic technique that uses ultrasound to estimate the stiffness of tissues by measuring the degree of distortion under application of an external force. Ultrasound elastography has mostly been applied to studies of liver and breast pathology [(45-48)]. In the thyroid gland, elastography has been used to study the hardness/elasticity of thyroid nodules to differentiate malignant from benign lesions [(40)(49, 50)]. There are several elastography techniques that use external compression, carotid artery pulsations, etc. [(51, 52)]. In one method (Sonoline Elegra, Siemens) strain images are built by measuring the local displacement induced by a compressive force applied to the tissue surface [(53)]. Field displacements are estimated by using a correlation technique that tracks the echo delay in segmented waveforms recorded before and after the quasistatic compression. Tissue compression is displayed as an image called an elastogram on which the hard areas appear dark and the soft areas appear bright [(54)]. Biomechanical tests on samples of excised tumour and normal thyroid gland tissue are performed to

validate the results of thyroid strain imaging and elastic modulus using a special equation. The values, expressed in kilopascals, for normal thyroid gland tissue, benign nodules and malignant nodules are presented in Table 5.

**Table 5 Elastography values for normal thyroid, benign nodules and malignant nodules.**

| | kPa* | Range (kPa) | Ratio* |
|---|---|---|---|
| Normal thyroid | 12.3±4.8 | 5.8–18.7 | |
| Benign nodule | 22.5±9.6 | 11.9–37.4 | 2.3±1.7 |
| Malignant nodule | 99.7±79.8 | 15.9– 590.4 | 8.8±4.6 |

Data are mean values ± standard deviations (range)

Another method used in clinical practice (Hitachi Medical Systems) acquires two ultrasonic images, before and after tissue compression by the probe, and tracks tissue displacement by assessing imaging beam propagation [(55)]. Dedicated software provides an accurate measurement of tissue distortion. The ultrasound elastogram is displayed over the B-mode image in a colour scale that ranges from red, for components with the greatest elastic strain (softest components) to blue, for those with no strain (hardest components).

The latest method, shear-elastography mode (Aixplorer, Supersonic), simultaneously uses ultrasound waves and shear waves to better characterise and quantify tissue stiffness. Shear wave velocity is directly related to the quantifiable measurement of tissue elasticity. The scanner can generate, capture and quantify the velocity of a shear wave by acquiring data much faster than conventional ultrasound technology. A quantitative colour coded map displaying local tissue elasticity for a large image region is produced in real-time. An easy to read colour scale indicates tissue elasticity in kilopascals, which are usually displayed in the range of 0–200kPa. Elastography images indicate local tissue elasticity as very soft (blue) and very hard (red) [Figure 47]. Note the difference in colour coding of elastography images in the Hitachi and Aixplorer systems. Figures 47 to 49 illustrate the elastographic features of different tissues using the Aixplorer, Supersonic shear wave elastography).

**Figure 47 Thyroid elastography. Very soft area (blue) and hard area (red).**

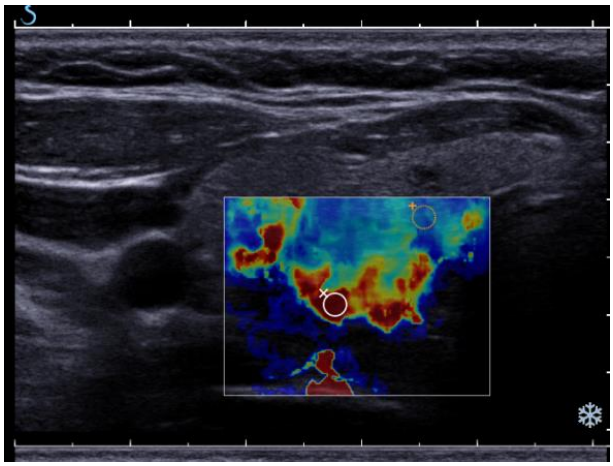

The technique requires no manual compression. Pulses are successively focused at different depths in tissue at supersonic speed. Shear wave propagation is captured with plane waves. Shear wave propagation speed relates directly to the local elasticity of tissue and can be measured in kilopascals. The so-called “Q-Box” quantification tool accurately measures, in real-time, true tissue elasticity in kilopascals by placing a region of interest (ROI) in the desired area. Multiple areas of interest can be compared and the ratio of stiffness between these areas measured (E-ratio) [Figure 48].

**Figure 48** **Goiterous benign nodule. The stiffness of the hypoechoic thyroid nodule is lower than the thyroid parenchyma (8.6kPa *vs* 13.5kPa; E-ratio, 0.6). Q-Box elastography compares the stiffness of the two regions as a ratio (nodule (large region of interest (ROI)) to parenchyma (small ROI)). Although the hypoechogenic nodule was morphologically moderately suspicious, elastography demonstrated a very soft nodule, which was softer than the surrounding parenchyma. FNA confirmed that the nodule was benign. Fine-needle aspiration demonstrates a nodular goitre (benign nodule).**

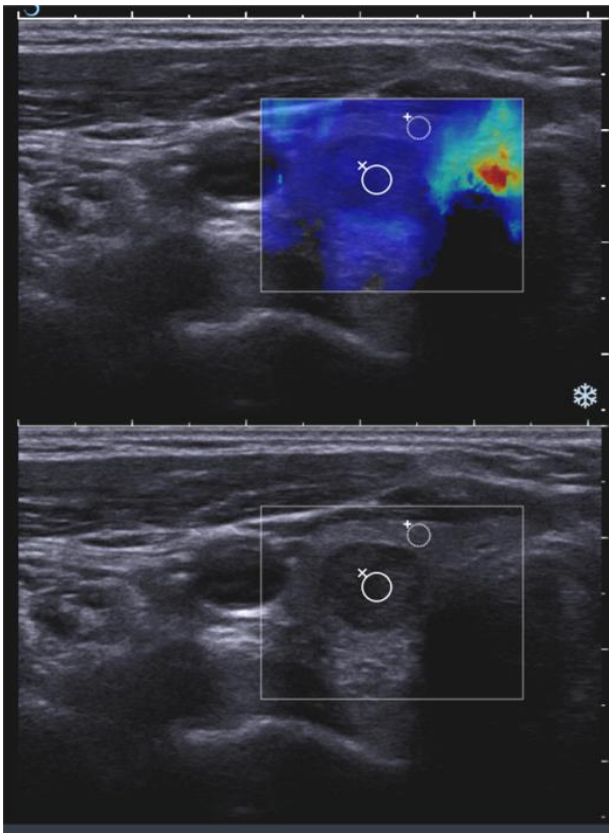

In Figure 49 the elastographic image of papillary cancer is presented. The nodule is quite hard (red on the colour display) and quantification of its elastic properties demonstrated that it is much harder than the surrounding thyroid gland parenchyma.

**Figure 49 Thyroid papillary cancer. The nodule is very stiff (red on colour display). The measured stiffness of the nodule is 102.1kPa, while adjacent normal parenchymal stiffness is 32/9kPA. An E-ratio of 5.1 indicates the cancer is 5 times harder than normal parenchyma.**

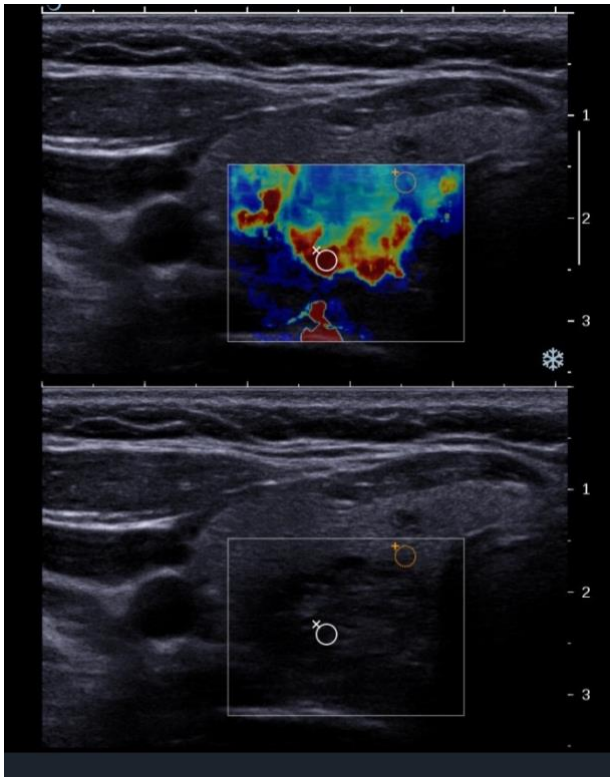


The elastographic presentation of Hürtle-cell tumour [Figure 50], simple thyroid cyst [Figure 51], thyroid cyst with solid component [Figure 52], calcifications within a thyroid nodule [Figure 53] and Hashimoto's thyroiditis [Figure 54] are illustrated.

**Figure 50** **Hürtle-cell tumour. A mixed solid and cystic nodule is seen. The Q-Box is positioned in the solid part of the tumour, which probably contains some calcifications. A very high stiffness value of 279.4kPa is measured, while the adjacent area of the tumour measures only 25.1kPa. The colour image displays these differences clearly with the hard area encoded in the red colour.**

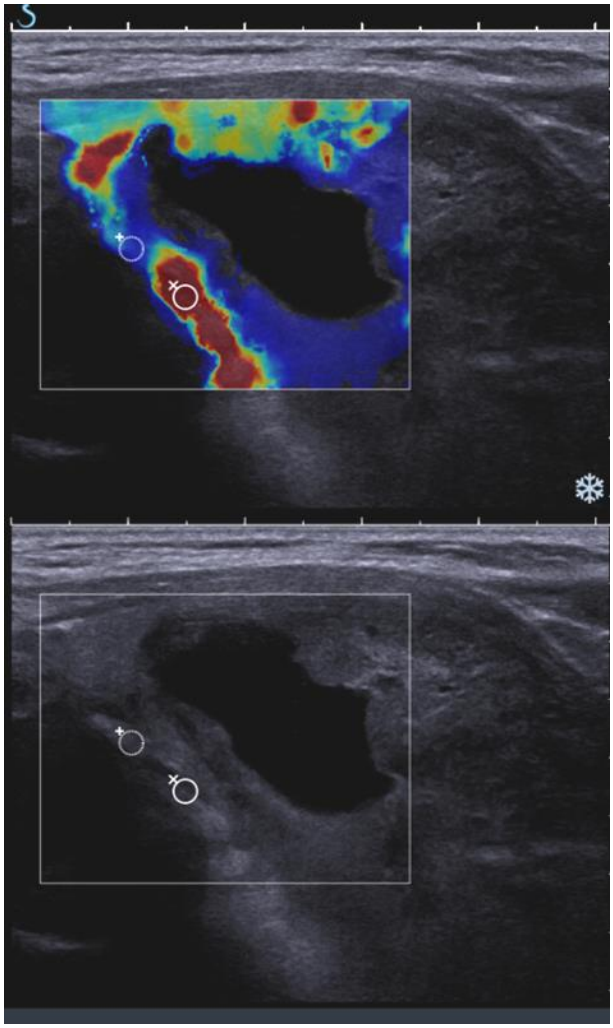

**Figure 51 Simple thyroid cyst. The Q-Box within the cyst measures 12.6kPa and in the normal parenchyma, which is slightly harder than the cyst, it measures 16.6kPa. The E-ratio is 0.8.**

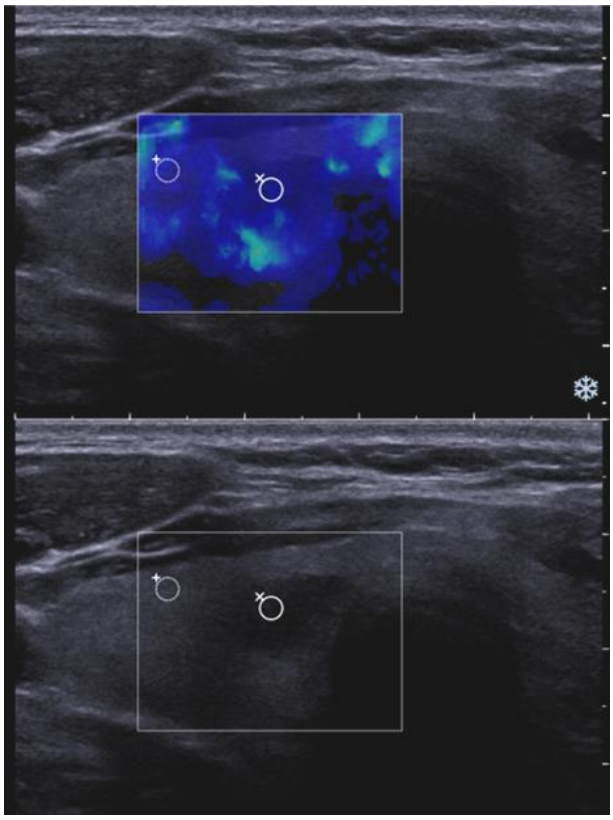

**Figure 52 Thyroid cyst with solid protrusion. The solid part within the cyst is harder (20.6kPa) compared with values in the liquid part of the cyst (12kPa).**

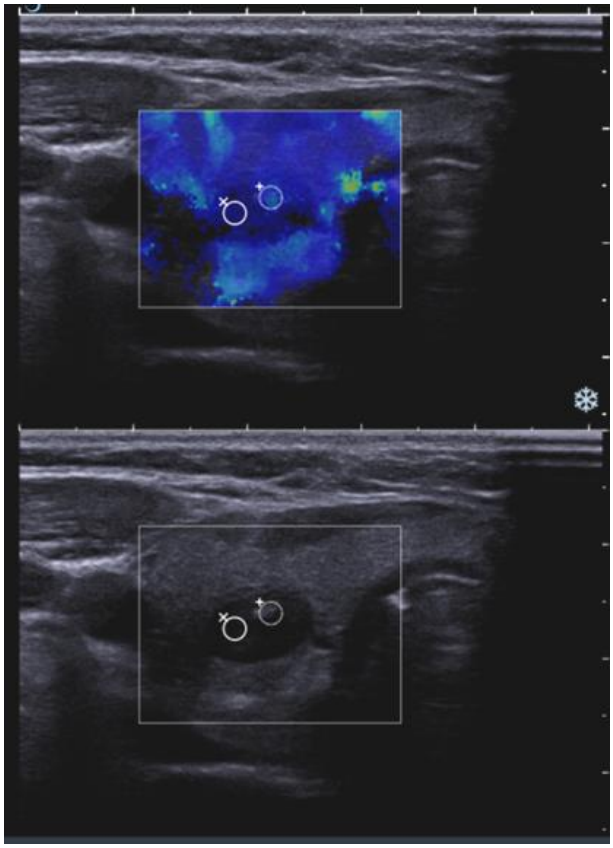

**Figure 53 Calcification within a nodule. The calcium deposit is very hard and appears in red. The Q-box is positioned at the edge of the calcification with a high stiffness of 217.3kPa.**

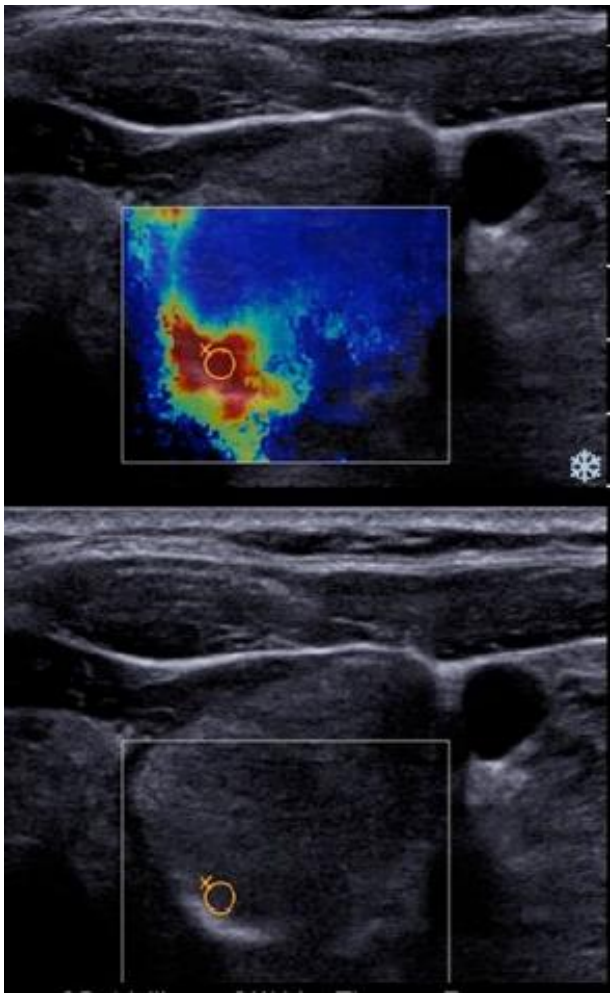

**Figure 54 Diffuse thyroid disease (Hashimoto's thyroiditis). The red colour represents tracheal cartilage. Measurements in two areas of the thyroid lobe are 17.5 and 18.4kPa.**

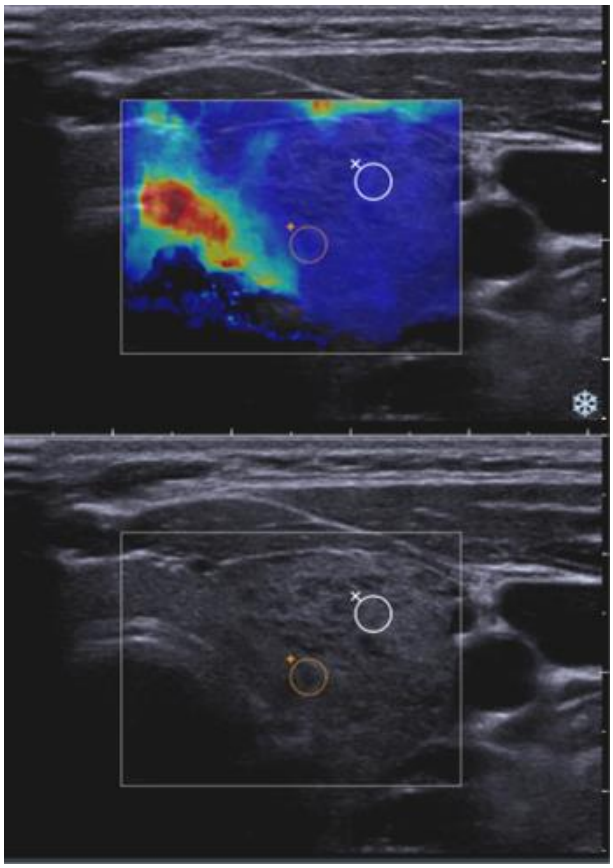

## Contrast-enhanced ultrasound

Contrast-enhanced ultrasound (CEUS) provides only ancillary data for the diagnosis of malignant thyroid nodules. Variation of time-intensity curves during the transit times of the injected microbubbles offers a modest improvement over the information obtained with traditional ultrasound, colour or power Doppler examinations. New specifically designed microbubbles and new models of ultrasound equipment with specific software are needed to improve the predictive value of CEUS for small parts application [(56-59)].

## Scintigraphy

Thyroid scintigraphy ($^{123}I$ or $^{99}TcO_4^m$) for a thyroid nodule or MNG is requested less nowadays because of the availability of ultrasound and the aggressive use of FNA in thyroid nodules. A normal thyroid scintigraphy shows homogeneous distribution of the radiotracer throughout the gland [Figure 55].

**Figure 55 Normal thyroid scintigraphy. A homogeneous distribution of the radiotracer throughout the gland is seen. Note oesophageal activity (arrow) on the left plot.**

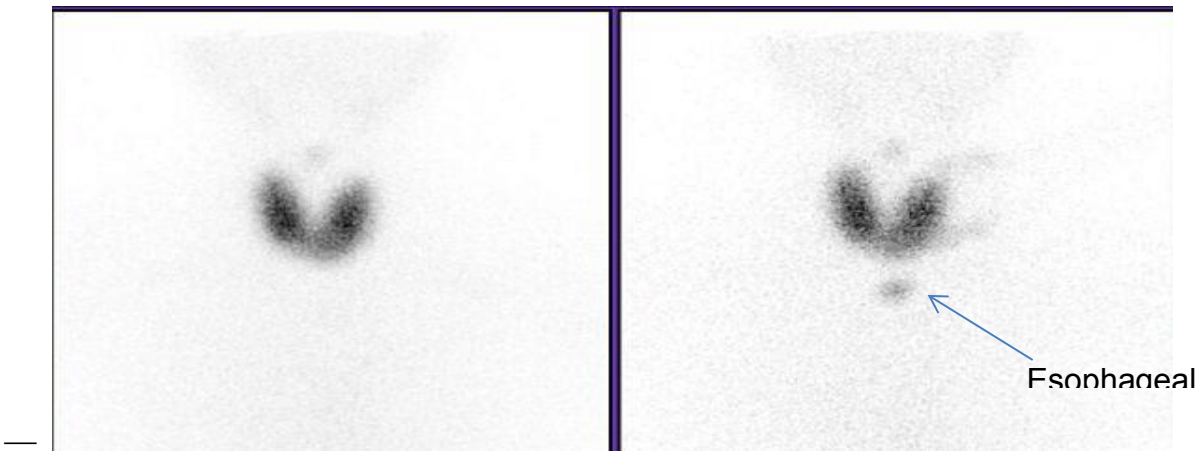


The clinical indications for thyroid scintigraphy, according to the American Association of Clinical Endocrinologists medical guidelines for clinical practice for the diagnosis and management of thyroid nodules [(18)], are TSH level below the normal range, iodine deficient areas even if the TSH level is in the low-normal range and suspected ectopic thyroid tissue or retrosternal goitre [Figure 56].

**Figure 56 Lingual thyroid. Ectopic thyroid tissue uptake at the level of the foramen caecum.**

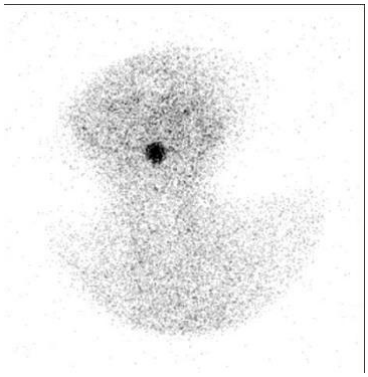

Findings on thyroid scintigraphy are unspecific. A cold nodule may represent a benign lesion (such as an adenoma, cyst or haemorrhage) or a malignant one (well-differentiated carcinoma, medullary or anaplastic carcinoma) [Figure 57]. Less than 20% of cold nodules are actually a malignant nodule. A hot nodule is generally an autonomous or hypertrophic adenoma [Figure 58].

**Figure 57 Cold nodule. Benign cold nodule on cytology (on the left). Malignant cold nodule on cytology (on the right). Scintigraphy is unspecific for the differentiation between benign and malignant cold nodules.**

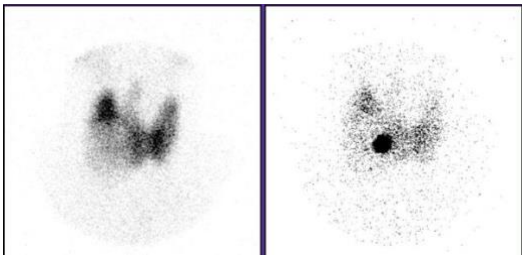

**Figure 58 Hot nodule. Single nodule in left lobe (on the left). Multiple nodules in both lobes (on the right). Note the retrosternal placement of the nodule in the right lobe. On cytology, autonomous or hypertrophic adenomas were diagnosed.**

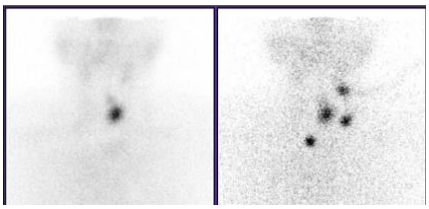

**Computed tomography**

CT is inferior to ultrasound in the differential diagnosis of thyroid nodules. The purpose of performing CT examination is largely limited to the pre-operative evaluation of tumours that are too large to be assessed by ultrasound alone in order to determine the presence of extracapsular or mediastinal invasion. CT also carries considerable radiation dose to the radiosensitive thyroid gland. Multidetector row CT (MDCT) provides higher spatial resolution than conventional CT scanners and allows the assessment of tumour extension on three-dimensional reformatted images with excellent image quality.

CT examination of the thyroid gland is performed according to a standard protocol. No contrast medium is administered for the thyroid, which is easily discriminated from its adjacent tissue owing to the high density of the gland, to avoid interference with hormonal function and radioiodine-related diagnostic tests or treatment. Image acquisition is done at 3mm thickness. Thin sections (1mm) are used for three-dimensional and multiplanar reconstructions (MPR). When indicated, 100ml of iodinated contrast medium is injected via an antecubital vein at a 4ml/s. Images are acquired in the arterial and late phases. MDCT provides accurate data on invasion of surrounding tissues, including muscles, trachea, oesophagus and blood vessels [Figure 59]. MDCT cannot distinguish between benign and malignant nodules. The dynamics of thyroid nodule contrast enhancement has not been studied in detail; however, differences in density have been observed between normal parenchyma and benign and malignant thyroid nodules in the late imaging phase.

On MPR morphological distortion of the trachea or oesophagus by thyroid tumours can be evaluated on multidirectional images. As these structures run in the craniocaudal direction, coronal and sagittal reformatted images are effective to observe compression or invasion by the tumour. Oblique sections in which the plane is free are particularly effective for evaluating tracheal invasion. With three-dimensional imaging, the entire thyroid gland can be observed at the same time and the number and location of nodules are easily determined. Three-dimensional imaging is also useful for the display of irregularity in the nodule surface and tracheal distortion.

**Figure 59 An inhomogeneous thyroid nodule with regular margins, internal cystic changes and small calcifications is seen in the left lobe. It is a benign nodule, which was diagnosed by ultrasound-guided fine-needle aspiration. The nodule is clearly delineated from the surrounding thyroid parenchyma, which can be seen in both benign and malignant nodules.**

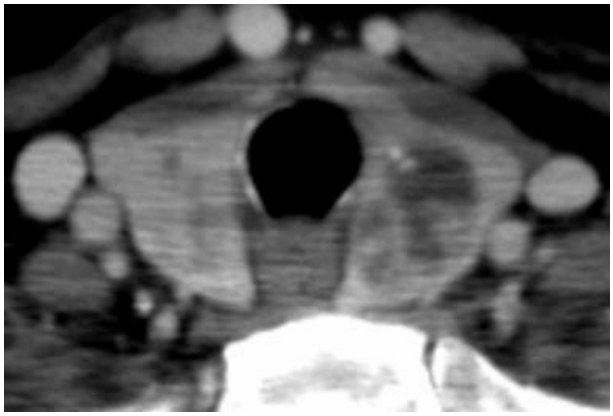

**Figure 60 Coronal multiplanar reconstructions through the thyroid nodule in the left lobe seen in the previous figure. The trachea is slightly compressed by the nodule and displaced towards the right side.**

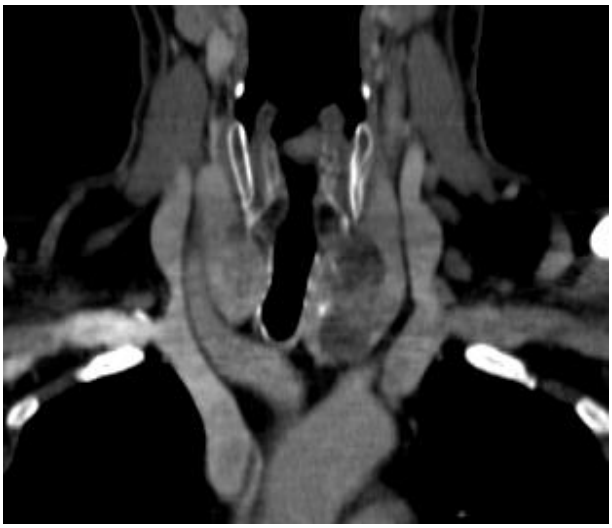

**Positron emission tomography**

Positron emission tomography (PET) is a rapidly evolving imaging modality that has gained widespread acceptance in oncology. There are several radionuclides applicable to thyroid cancer. Thyroid cancer patients are commonly studied using 18F-Fluorodeoxyglucose (FDG-PET). Perhaps the greatest use being the potential to localise the tumour in DTC patients who are radioiodine whole body scan (WBS) negative and thyroglobulin (Tg) positive. Several studies have evaluated sensitivity and specificity of FDG accumulation in thyroid cancer. Some studies demonstrated FDG accumulation in all cancers, while other studies showed an accumulation in benign nodules as well as in malignant nodules. In conclusion, FDG-PET is useful in patients in whom the FNA results are inconclusive and positive accumulation on PET indicates probable cancer and the need for surgery. Emerging data suggest that PET/CT fusion studies provide increased accuracy and modify the treatment plan in a significant number of DTC cases when compared with PET images alone [(60)].

### Magnetic resonance imaging (MRI)

To date, little information is available on the use of MRI in the diagnosis of thyroid cancer. The conventional MRI protocol includes $T_1$ weighted spin-echo imaging, $T_2$ weighted fast spin-echo imaging and inversion recovery imaging [(61)]. Cystic areas of the lesion are defined by characteristic $T_1$ and $T_2$ weighted images and correlate with sonographic findings. Recently, diffusion-weighted imaging (DWI) has evolved as a helpful diagnostic tool for assessing tumour characterisation, not only in neural but also extraneural lesions, such as bone marrow pathologies, lymph nodes and liver tumours. DWI is based on the random translational motion of water protons, which reflects the tissue-specific diffusion capacity. The diffusion capacity is indirectly proportional to diffusion barriers. Structural changes characteristic of malignancies or benign tissue result in different signals on DWI, which may be quantified by calculating the apparent diffusion coefficient (ADC). In general, rapidly growing tumours are characterised by increased cell attenuation and increased amount of diffusion barriers [(62)]. The initial results indicate that DWI has the potential to enable differentiation between thyroid carcinoma, adenoma and normal parenchyma [(3, 62)]. Dynamic contrast-enhanced MRI (DCE-MRI) is useful in differentiating malignant and benign lesions of brain, breast, endometrium and salivary glands. Thyroid carcinoma or thyroid nodules with a high cell proliferation index demonstrate delayed washout pattern on DCE-MRI [(63)]. DCE-MRI is useful in the detection or exclusion of thyroid carcinoma with high diagnostic accuracy in patients with MNG when results of other diagnostic methods are inconclusive [(64)].

## Diagnostic algorithm

FNA cytology is the most important test in the management of thyroid nodules. FNA has an 85% (65–98% range) sensitivity, 99% (72–100% range) specificity and 95% overall accuracy for the diagnosis of focal thyroid lesions (65). FNA can be performed blindly by palpation or ultrasound-guided to increase confidence, if the lesion is palpable. In addition, ultrasound-guided FNA can be used to help localise non-palpable lesions, lesions less than 1cm or when initial free-hand FNA was non-diagnostic. Experienced cytologists should evaluate the

specimen. Core biopsy should be considered after two aspiration procedures showing non-diagnostic specimen or when thyroid lymphoma is suspected.

Ultrasound allows the detection of thyroid and cervical masses, gross differentiation of benign from malignant masses based on imaging features and guidance for FNA biopsy and percutaneous treatment. Ultrasound can accurately document the size of a thyroid swelling and therefore, because it is non-invasive, serial scans may be performed, which allow better assessment of growth.

CT and MRI are indicated in selected cases to determine staging and local extent of the diseases for planning surgery. CT and MRI are indicated when there is a potential infiltration of surrounding tissues by the thyroid mass. Other important indications include cervical lymphadenopathy or cases when the limits of the goitre cannot be determined clinically or by ultrasound, such as retrosternal goitre. CT and MRI can demonstrate involvement of the larynx, pharynx, trachea, oesophagus or major blood vessels. MRI is used to plan surgical procedures in patients with symptoms of extrathyroidal tumour extension (usually voice change or dysphagia). MR is better than CT for evaluating the relationship of tumour to the larynx, oesophagus, trachea, spine and major vessels both prior to thyroidectomy and at local regional recurrence. It is important to avoid iodine contrast media in CT to ensure that subsequent radioiodine treatment uptake by the remaining thyroid tissue is not compromised. This difficulty may be overcome by a gadolinium-enhanced MRI scan. In the majority of cases a CT or MR scan is not performed prior to thyroidectomy. In the absence of symptoms of tumour invasion of adjacent structures, pre-operative CT or MRI does not add useful information. It is not necessary to obtain a CT or MR scan to look for adenopathy prior to thyroidectomy. Unlike other head and neck malignancies, it is not necessary to stage the neck with CT or MR scans. The extent of node dissection is determined by cervical ultrasonography and palpation of the nodes.

PET-CT has a significant role in the overall post-surgery management especially in patients with elevated serum thyroglobulin (Tg) but negative radioiodine WBSs. PET-CT should be a part of the routine tests in the Tg positive/radioiodine scan negative patient [(66)].

In conclusion, ultrasound should be the first imaging test in the clinical work-up of a patient with suspicion of thyroid pathology. When ultrasound demonstrates a nodule suspicious for malignancy or there is a history of radiation, MEN II type or thyroidectomy, FNA should be the second diagnostic examination either by palpation or under ultrasound-guidance.

In pre-operative planning, CT or MRI should be performed in the presence of symptoms of tumour invasion of adjacent structures.

## Conclusion

The main advantages of thyroid sonography:

- ability to detect thyroid and cervical masses and to differentiate between probably benign and probably malignant masses based on sonographic criteria;
- papillary thyroid tumour is the most prevalent type of thyroid cancer and generally has a favourable prognosis; and
- ability to guide FNA biopsy and percutaneous treatment of thyroid nodules.

Main limitations of thyroid sonography:

- some overlapping in sonographic features of benign and malignant masses;
- difficult identification of suspected lesions in MNG; and
- operator and equipment quality dependant.

## References

1. Haugen BR, Alexander EK, Bible KC, Doherty GM, Mandel SJ, Nikiforov YE, Pacini F, et al. 2015 American Thyroid Association Management Guidelines for Adult Patients with Thyroid Nodules and Differentiated Thyroid Cancer: The American Thyroid Association Guidelines Task Force on Thyroid Nodules and Differentiated Thyroid Cancer. Thyroid 2016;26:1-133.

2. Tessler FN, Middleton WD, Grant EG, Hoang JK, Berland LL, Teefey SA, Cronan JJ, et al. ACR Thyroid Imaging, Reporting and Data System (TI-RADS): White Paper of the ACR TI-RADS Committee. J Am Coll Radiol 2017;14:587-595.

3. Sundram FX. Clinical use of PET/CT in thyroid cancer diagnosis and management. Biomed Imaging Interv J 2006;2:e56.

4. Ahuja A, Chick W, King W, Metreweli C. Clinical significance of the comet-tail artifact in thyroid ultrasound. J Clin Ultrasound 1996;24:129-133.

5. Kim MJ, Kim EK, Kwak JY, Park CS, Chung WY, Nam KH, Youk JH. Differentiation of thyroid nodules with macrocalcifications: role of suspicious sonographic findings. J Ultrasound Med 2008;27:1179-1184.

6. Kwak JY, Han KH, Yoon JH, Moon HJ, Son EJ, Park SH, Jung HK, et al. Thyroid imaging reporting and data system for US features of nodules: a step in establishing better stratification of cancer risk. Radiology 2011;260:892-899.

7. Na DG, Kim DS, Kim SJ, Ryoo JW, Jung SL. Thyroid nodules with isolated macrocalcification: malignancy risk and diagnostic efficacy of fine-needle aspiration and core needle biopsy. Ultrasonography 2016;35:212-219.

8. Taki S, Terahata S, Yamashita R, Kinuya K, Nobata K, Kakuda K, Kodama Y, et al. Thyroid calcifications: sonographic patterns and incidence of cancer. Clin Imaging 2004;28:368-371.

9. Arpaci D, Ozdemir D, Cuhaci N, Dirikoc A, Kilicyazgan A, Guler G, Ersoy R, et al. Evaluation of cytopathological findings in thyroid nodules with macrocalcification: macrocalcification is not innocent as it seems. Arq Bras Endocrinol Metabol 2014;58:939-945.

10. McIvor NP, Freeman JL, Salem S. Ultrasonography of the thyroid and parathyroid glands. ORL J Otorhinolaryngol.Relat Spec. 1993;55:303-308.

11. Cochand-Priollet B, Guillausseau PJ, Chagnon S, Hoang C, Guillausseau-Scholer C, Chanson P, Dahan H, et al. The diagnostic value of fine-needle aspiration biopsy under ultrasonography in nonfunctional thyroid nodules: a prospective study comparing cytologic and histologic findings. Am J Med 1994;97:152-157.

12. Marqusee E, Benson CB, Frates MC, Doubilet PM, Larsen PR, Cibas ES, Mandel SJ. Usefulness of ultrasonography in the management of nodular thyroid disease. Ann Intern Med 2000;133:696-700.

13. Papini E, Guglielmi R, Bianchini A, Crescenzi A, Taccogna S, Nardi F, Panunzi C, et al. Risk of malignancy in nonpalpable thyroid nodules: predictive value of ultrasound and color-Doppler features. J Clin Endocrinol Metab 2002;87:1941-1946.

14. Cochand-Priollet B, Guillausseau PJ, Chagnon S, Hoang C, Guillausseau-Scholer C, Chanson P, Dahan H, et al. The diagnostic value of fine-needle aspiration biopsy under ultrasonography in nonfunctional thyroid nodules: a prospective study comparing cytologic and histologic findings. Am.J Med 1994;97:152-157.

15. Marqusee E, Benson CB, Frates MC, Doubilet PM, Larsen PR, Cibas ES, Mandel SJ. Usefulness of ultrasonography in the management of nodular thyroid disease. Ann.Intern.Med 2000;133:696-700.

16. Papini E, Guglielmi R, Bianchini A, Crescenzi A, Taccogna S, Nardi F, Panunzi C, et al. Risk of malignancy in nonpalpable thyroid nodules: predictive value of ultrasound and color-Doppler features. J Clin Endocrinol.Metab 2002;87:1941-1946.

17. Propper RA, Skolnick ML, Weinstein BJ, Dekker A. The nonspecificity of the thyroid halo sign. J Clin Ultrasound 1980;8:129-132.

18. Moon HJ, Kwak JY, Kim EK, Kim MJ. A taller-than-wide shape in thyroid nodules in transverse and longitudinal ultrasonographic planes and the prediction of malignancy. Thyroid 2011;21:1249-1253.

19. Lagalla R, Cariso G, Midiri M. Echo Doppler couleur et pathologie thyroidienne. J Echograph Med Ultrasons 1992;13:44-47.

20. Davies L, Welch HG. Increasing incidence of thyroid cancer in the United States, 1973-2002. JAMA 2006;295:2164-2167.

21. Papini E, Guglielmi R, Bianchini A, Crescenzi A, Taccogna S, Nardi F, Panunzi C, et al. Risk of malignancy in nonpalpable thyroid nodules: predictive value of ultrasound and color-Doppler features. J Clin Endocrinol. Metab 2002;87:1941-1946.

22. Fagin JA, Mitsiades N. Molecular pathology of thyroid cancer: diagnostic and clinical implications. Best Pract Res Clin Endocrinol Metab 2008;22:955-969.

23. Shin LK, Olcott EW, Jeffrey RB, Desser TS. Sonographic evaluation of cervical lymph nodes in papillary thyroid cancer. Ultrasound Q 2013;29:25-32.

24. Schlumberger M, Berg G, Cohen O, Duntas L, Jamar F, Jarzab B, Limbert E, et al. Follow-up of low-risk patients with differentiated thyroid carcinoma: a European perspective. Eur J Endocrinol. 2004;150:105-112.

25. Leboulleux S, Girard E, Rose M, Travagli JP, Sabbah N, Caillou B, Hartl DM, et al. Ultrasound criteria of malignancy for cervical lymph nodes in patients followed up for differentiated thyroid cancer. J Clin Endocrinol Metab 2007;92:3590-3594.

26. Kim DW, Choo HJ, Lee YJ, Jung SJ, Eom JW, Ha TK. Sonographic features of cervical lymph nodes after thyroidectomy for papillary thyroid carcinoma. J Ultrasound Med 2013;32:1173-1180.

27. Leboulleux S, Rubino C, Baudin E, Caillou B, Hartl DM, Bidart JM, Travagli JP, et al. Prognostic factors for persistent or recurrent disease of papillary thyroid carcinoma with neck lymph node metastases and/or tumor extension beyond the thyroid capsule at initial diagnosis. J Clin Endocrinol Metab 2005;90:5723-5729.

28. Spencer C, Fatemi S, Singer P, Nicoloff J, Lopresti J. Serum Basal thyroglobulin measured by a second-generation assay correlates with the recombinant human thyrotropin-stimulated thyroglobulin response in patients treated for differentiated thyroid cancer. Thyroid 2010;20:587-595.

29. Cappelli C, Pirola I, Gandossi E, De Martino E, Agosti B, Castellano M. Fine-needle aspiration cytology of thyroid nodule: does the needle matter? South. Med J 2009;102:498-501.

30. Frates MC, Benson CB, Charboneau JW, Cibas ES, Clark OH, Coleman BG, Cronan JJ, et al. Management of thyroid nodules detected at US: Society of Radiologists in Ultrasound consensus conference statement. Radiology 2005;237:794-800.

31. Park JY, Lee HJ, Jang HW, Kim HK, Yi JH, Lee W, Kim SH. A proposal for a thyroid imaging reporting and data system for ultrasound features of thyroid carcinoma. Thyroid 2009;19:1257-1264.

32. Horvath E, Majlis S, Rossi R, Franco C, Niedmann JP, Castro A, Dominguez M. An ultrasonogram reporting system for thyroid nodules stratifying cancer risk for clinical management. J Clin Endocrinol Metab 2009;94:1748-1751.

33. Rago T, Santini F, Scutari M, Pinchera A, Vitti P. Elastography: new developments in ultrasound for predicting malignancy in thyroid nodules. J Clin Endocrinol. Metab 2007;92:2917-2922.

34. Cibas ES, Ali SZ. The Bethesda System for Reporting Thyroid Cytopathology. Thyroid 2009;19:1159-1165.

35. Cibas ES, Ali SZ, Conference NCITFSotS. The Bethesda System For Reporting Thyroid Cytopathology. Am J Clin Pathol 2009;132:658-665.

36. Cibas ES, Ali SZ. The 2017 Bethesda System for Reporting Thyroid Cytopathology. Thyroid 2017;27:1341-1346.

37. Cibas ES, Ali SZ. The 2017 Bethesda System for Reporting Thyroid Cytopathology. J Am Soc Cytopathol 2017;6:217-222.

38. Ali SZ, Cibas ES. The Bethesda System for Reporting Thyroid Cytopathology II. Acta Cytol 2016;60:397-398.

39. Yoon JH, Lee HS, Kim EK, Moon HJ, Kwak JY. Thyroid Nodules: Nondiagnostic Cytologic Results according to Thyroid Imaging Reporting and Data System before and after Application of the Bethesda System. Radiology 2015;276:579-587.

40. Gao L, Xi X, Wang J, Yang X, Wang Y, Zhu S, Lai X, et al. Ultrasound risk evaluation of thyroid nodules that are "unspecified" in the 2015 American Thyroid Association management guidelines: A retrospective study. Medicine (Baltimore) 2018;97:e13914.

41. Middleton WD, Teefey SA, Reading CC, Langer JE, Beland MD, Szabunio MM, Desser TS. Comparison of Performance Characteristics of American College of Radiology TI-RADS, Korean Society of Thyroid Radiology TIRADS, and American Thyroid Association Guidelines. AJR Am J Roentgenol 2018;210:1148-1154.

42. Eng CY, Quraishi MS, Bradley PJ. Management of Thyroid nodules in adult patients. Head Neck Oncol. 2010;2:11.

43. Tewfik TL, Yoskovitch A: Thyroglossal Duct Cysts/Ectopic Thyroid. In: Neck E, ed. Congenital Malformations, 2010.

44. O'Brien T, Gharib H, Suman VJ, van Heerden JA. Treatment of toxic solitary thyroid nodules: surgery versus radioactive iodine. Surgery 1992;112:1166-1170.

45. Dietrich CF, Bamber J, Berzigotti A, Bota S, Cantisani V, Castera L, Cosgrove D, et al. EFSUMB Guidelines and Recommendations on the Clinical Use of Liver Ultrasound Elastography, Update 2017 (Long Version). Ultraschall Med 2017;38:e48.

46. Shiina T, Nightingale KR, Palmeri ML, Hall TJ, Bamber JC, Barr RG, Castera L, et al. WFUMB guidelines and recommendations for clinical use of ultrasound elastography: Part 1: basic principles and terminology. Ultrasound Med Biol 2015;41:1126-1147.

47. Barr RG, Nakashima K, Amy D, Cosgrove D, Farrokh A, Schafer F, Bamber JC, et al. WFUMB guidelines and recommendations for clinical use of ultrasound elastography: Part 2: breast. Ultrasound Med Biol 2015;41:1148-1160.

48. Cosgrove D, Piscaglia F, Bamber J, Bojunga J, Correas JM, Gilja OH, Klauser AS, et al. EFSUMB guidelines and recommendations on the clinical use of ultrasound elastography. Part 2: Clinical applications. Ultraschall Med 2013;34:238-253.

49. Saftoiu A, Gilja OH, Sidhu PS, Dietrich CF, Cantisani V, Amy D, Bachmann-Nielsen M, et al. The EFSUMB Guidelines and Recommendations for the Clinical Practice of Elastography in Non-Hepatic Applications: Update 2018. Ultraschall Med 2019.

50. Cantisani V, David E, Grazhdani H, Rubini A, Radzina M, Dietrich CF, Durante C, et al. Prospective Evaluation of Semiquantitative Strain Ratio and Quantitative 2D Ultrasound Shear Wave Elastography (SWE) in Association with TIRADS Classification for Thyroid Nodule Characterization. Ultraschall Med 2019.

51. Dighe M, Bae U, Richardson ML, Dubinsky TJ, Minoshima S, Kim Y. Differential diagnosis of thyroid nodules with US elastography using carotid artery pulsation. Radiology 2008;248:662-669.

52. Dietrich CF, Barr RG, Farrokh A, Dighe M, Hocke M, Jenssen C, Dong Y, et al. Strain Elastography - How To Do It? Ultrasound Int Open 2017;3:E137-E149.

53. Lyshchik A, Higashi T, Asato R, Tanaka S, Ito J, Mai JJ, Pellot-Barakat C, et al. Thyroid gland tumor diagnosis at US elastography. Radiology 2005;237:202-211.

54. Dietrich CF, Bibby E, Jenssen C, Saftoiu A, Iglesias-Garcia J, Havre RF. EUS elastography: How to do it? Endosc Ultrasound 2018;7:20-28.

55. Rago T, Santini F, Scutari M, Pinchera A, Vitti P. Elastography: new developments in ultrasound for predicting malignancy in thyroid nodules. J Clin Endocrinol.Metab 2007;92:2917-2922.

56. Gharib H, Papini E, Valcavi R, Baskin HJ, Crescenzi A, Dottorini ME, Duick DS, et al. American Association of Clinical Endocrinologists and Associazione Medici Endocrinologi medical guidelines for clinical practice for the diagnosis and management of thyroid nodules. Endocr.Pract 2006;12:63-102.

57. Trimboli P, Dietrich CF, David E, Mastroeni G, Ventura Spagnolo O, Sidhu PS, Letizia C, et al. Ultrasound and ultrasound-related techniques in endocrine diseases. Minerva Endocrinol 2018;43:333-340.

58. Sidhu PS, Cantisani V, Dietrich CF, Gilja OH, Saftoiu A, Bartels E, Bertolotto M, et al. The EFSUMB Guidelines and Recommendations for the Clinical Practice of Contrast-Enhanced Ultrasound (CEUS) in Non-Hepatic Applications: Update 2017 (Short Version). Ultraschall Med 2018;39:154-180.

59. Sidhu PS, Cantisani V, Dietrich CF, Gilja OH, Saftoiu A, Bartels E, Bertolotto M, et al. The EFSUMB Guidelines and Recommendations for the Clinical Practice of Contrast-Enhanced

Ultrasound (CEUS) in Non-Hepatic Applications: Update 2017 (Long Version). Ultraschall Med 2018;39:e2-e44.

60. Hall NC, Kloos RT. PET imaging in differentiated thyroid cancer: where does it fit and how do we use it? Arq Bras.Endocrinol.Metabol. 2007;51:793-805.

61. Tezelman S, Giles Y, Tunca F, Gok K, Poyanli A, Salmaslioglu A, Terzioglu T. Diagnostic value of dynamic contrast medium enhanced magnetic resonance imaging in preoperative detection of thyroid carcinoma. Arch.Surg 2007;142:1036-1041.

62. Herneth AM, Friedrich K, Weidekamm C, Schibany N, Krestan C, Czerny C, Kainberger F. Diffusion weighted imaging of bone marrow pathologies. Eur J Radiol. 2005;55:74-83.

63. Kusunoki T, Murata K, Nishida S, Tomura T, Inoue M. Histopathological findings of human thyroid tumors and dynamic MRI. Auris Nasus Larynx 2002;29:357-360.

64. Tessler FN, Tublin ME. Thyroid sonography: current applications and future directions. AJR Am.J Roentgenol. 1999;173:437-443.

65. Dietrich CF, Muller T, Bojunga J, Dong Y, Mauri G, Radzina M, Dighe M, et al. Statement and Recommendations on Interventional Ultrasound as a Thyroid Diagnostic and Treatment Procedure. Ultrasound Med Biol 2018;44:14-36.

66. Waye JS, Eng B, Patterson M, Walker L, Carcao MD, Olivieri NF, Chui DH. Hemoglobin H (Hb H) disease in Canada: molecular diagnosis and review of 116 cases. Am.J Hematol. 2001;68:11-15.